Data analysis and numerical modelling of laser-plasma instabilities in a NIF shock ignition experiment

A. Ruocco,[1] K. Glize,[2] S. Morris,[3], T. Arber,[3], T. Goffrey,[3] K. Bennet[3], SJ Spencer,[4] and R. H. H. Scott[1]

[1] Central Laser Facility, STFC Rutherford Appleton Laboratory, Oxford, UK
[2] Shanghai Jiao Tong University
[3] University of Warwick
[4] UCLA

Planar experiments study LPI in ICF ignition regime

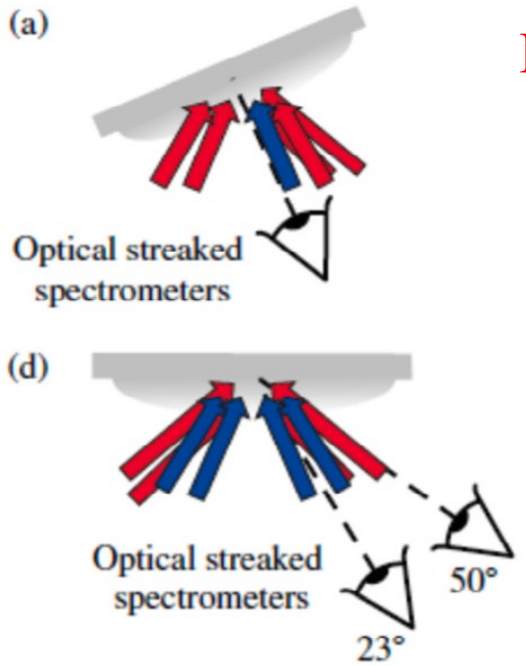

$L_n > 500$ um – $T_e > 4$ keV - $I_0 = 10^{15}$ W/ cm^2

Planar experiments study LPI in ICF ignition regime

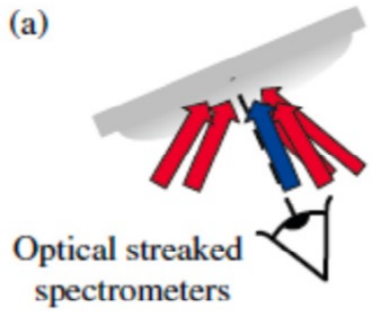

$L_n > 500$ um – $T_e > 4$ keV - $I_0 = 10^{15}$ W/ cm^2

Backward Raman Scattering (bSRS)

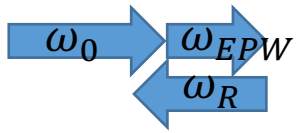

$$\omega_0 = \omega_{EPW} - \omega_R$$
$$k_0 = k_{EPW} - k_R$$

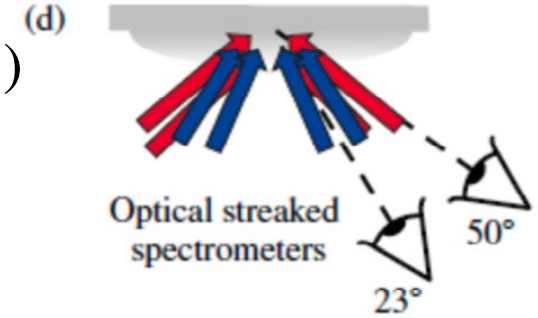

Planar experiments study LPI in ICF ignition regime

$L_n > 500$ um – $T_e > 4$ keV - $I_0 = 10^{15}$ W/ cm^2

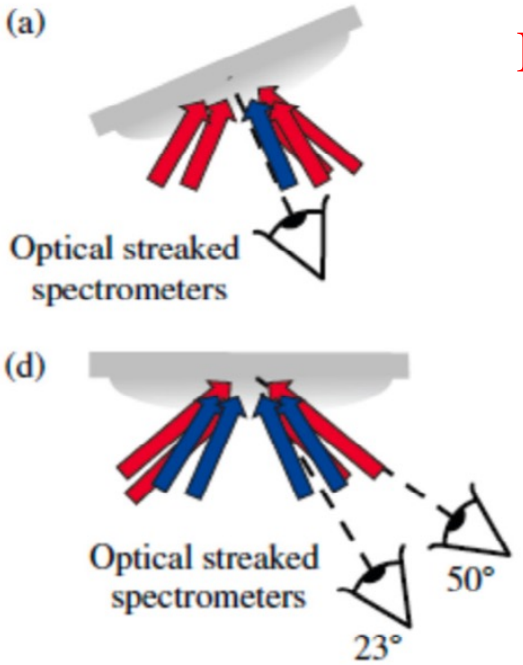

Backward Raman Scattering (bSRS)

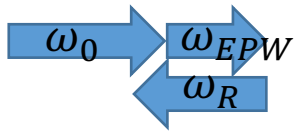

$$\omega_0 = \omega_{EPW} - \omega_R$$
$$k_0 = k_{EPW} - k_R$$

Side-scattered Raman (sSRS)

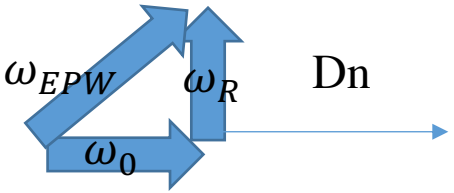

$$\boldsymbol{k}_0 = \boldsymbol{k}_{EPW} + \boldsymbol{k}_R$$

Planar experiments study LPI in ICF ignition regime

$L_n > 500$ um – $T_e > 4$ keV - $I_0 = 10^{15}$ W/ cm^2

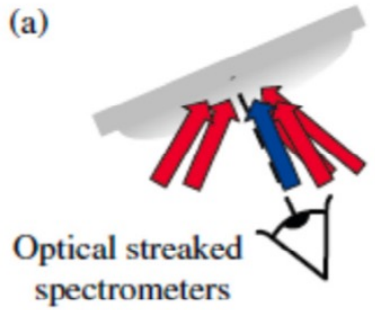

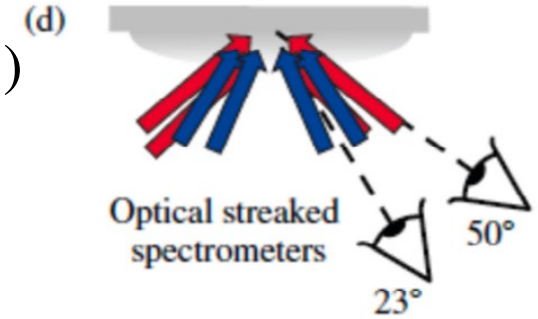

Backward Raman Scattering (bSRS)

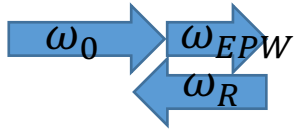

$\omega_0 = \omega_{EPW} - \omega_R$

$k_0 = k_{EPW} - k_R$

Side-scattered Raman (sSRS)

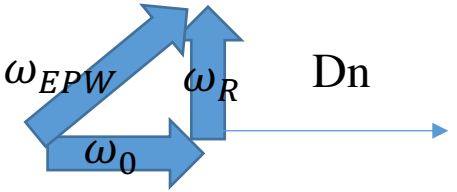

$\boldsymbol{k_0} = \boldsymbol{k_{EPW}} + \boldsymbol{k_R}$

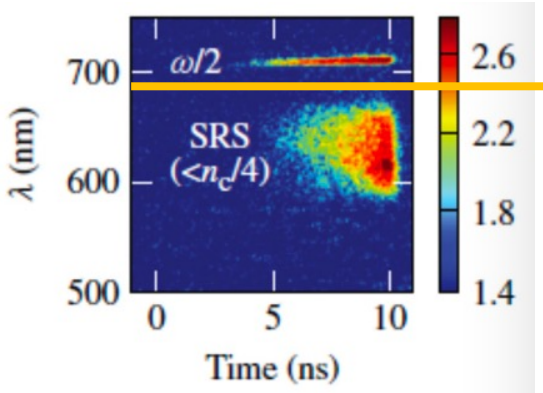

Broad

Low wavelength emission

Low density plasma

Narrow

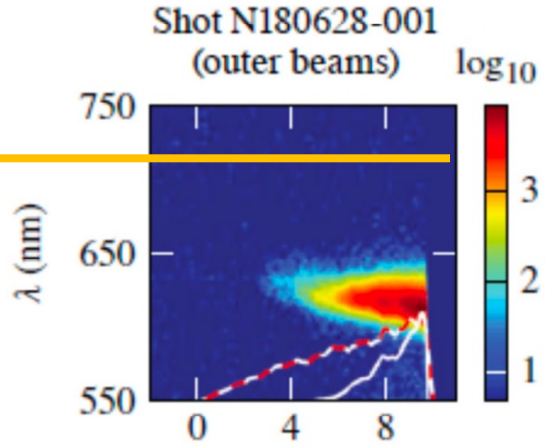

Rosenberg, PoP **27**, 042705 (2020)

N19 NIF experiment investigates LPI at shock-ignition conditions

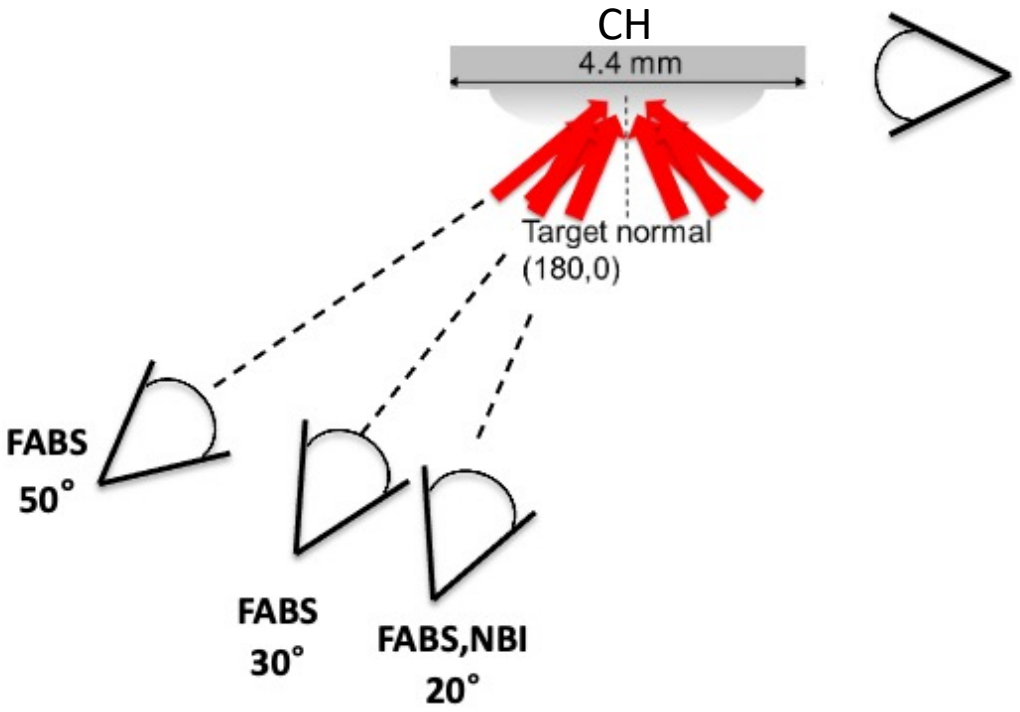

Xray spectrometer

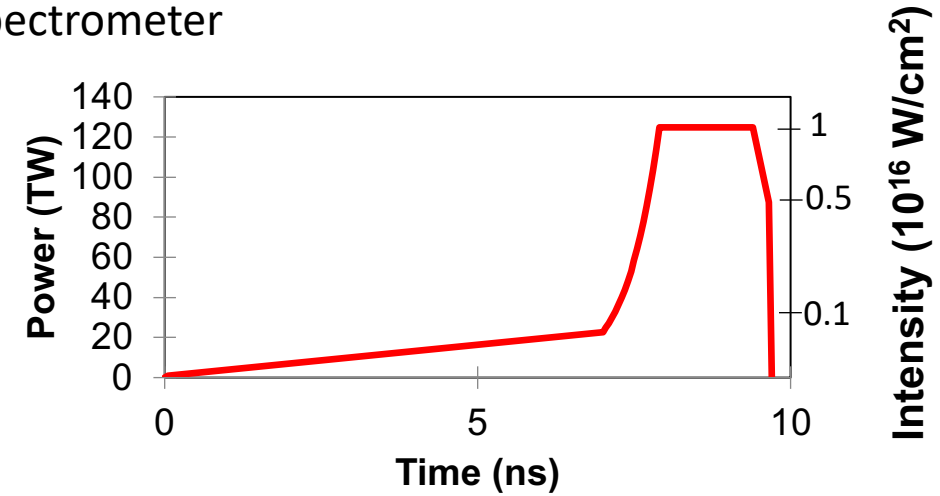

N19 NIF experiment investigates LPI at shock-ignition conditions

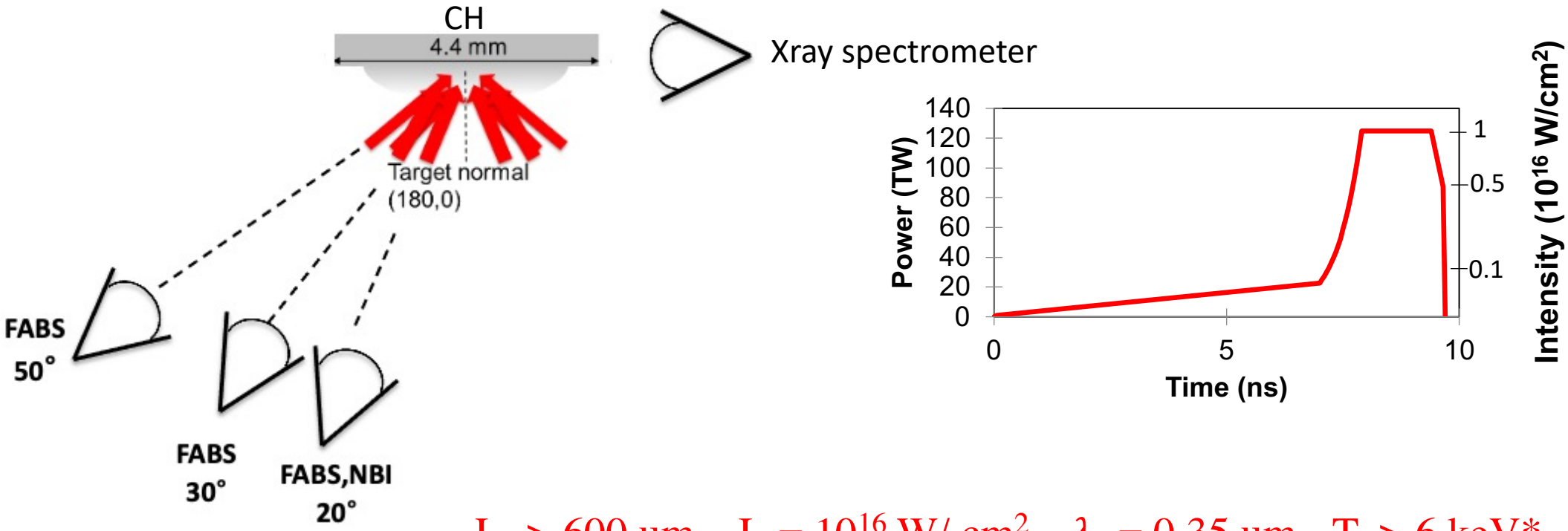

$L_n > 600$ um – $I_0 = 10^{16}$ W/ cm^2 – $\lambda_0 = 0.35$ um - $T_e > 6$ keV*

*hydrosimulations

Data analysis

Light diagnostics: FABS, NBI and diodes
Hot electron diagnostics: Xray spectrometer

Raman reflectivity not correlated with high hot electron production

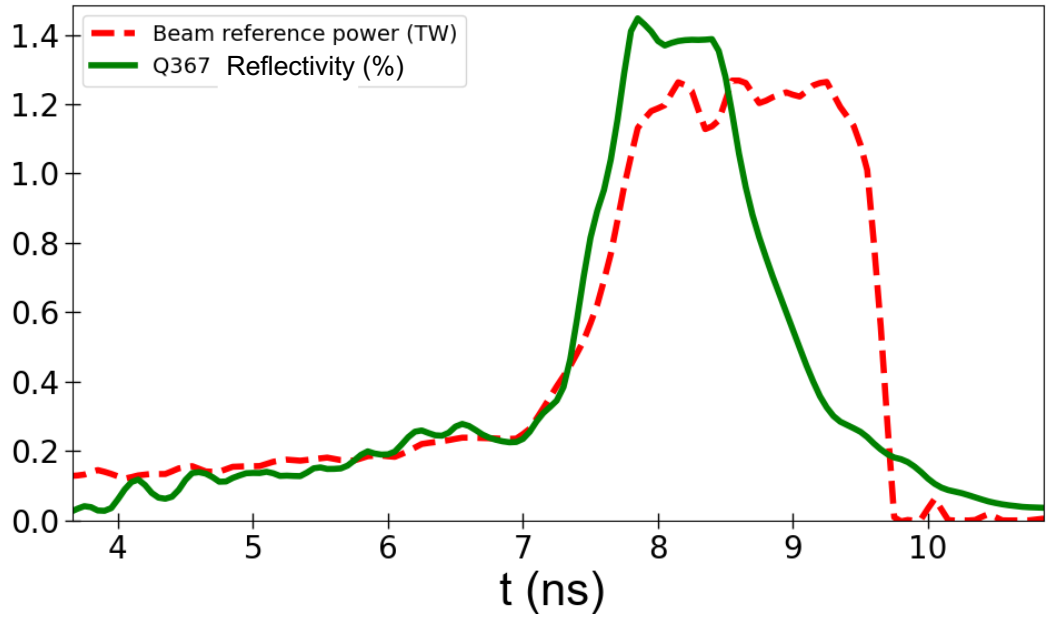

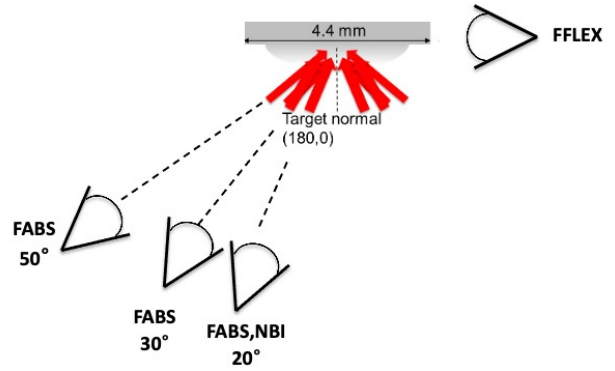

Time-integrated Raman reflectivity below 1%
HE conversion efficiency 12% - HE temperature 52 keV

FABS suggests dependence of Raman emission on observation angle

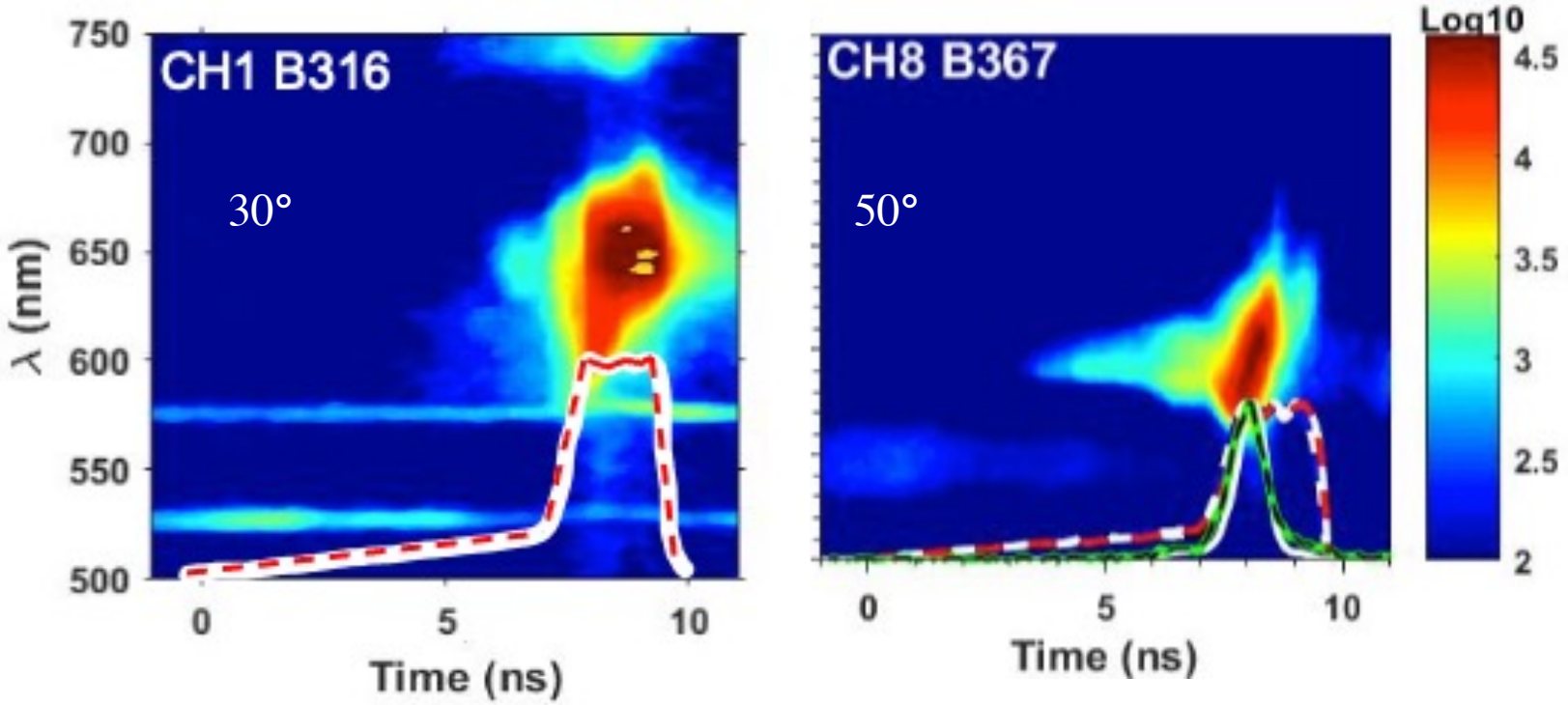

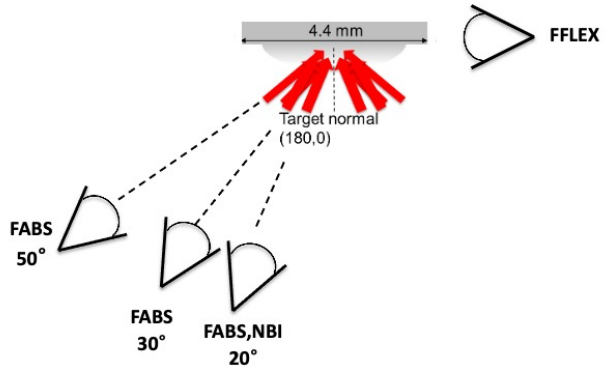

FABS suggests dependence of Raman emission on observation angle

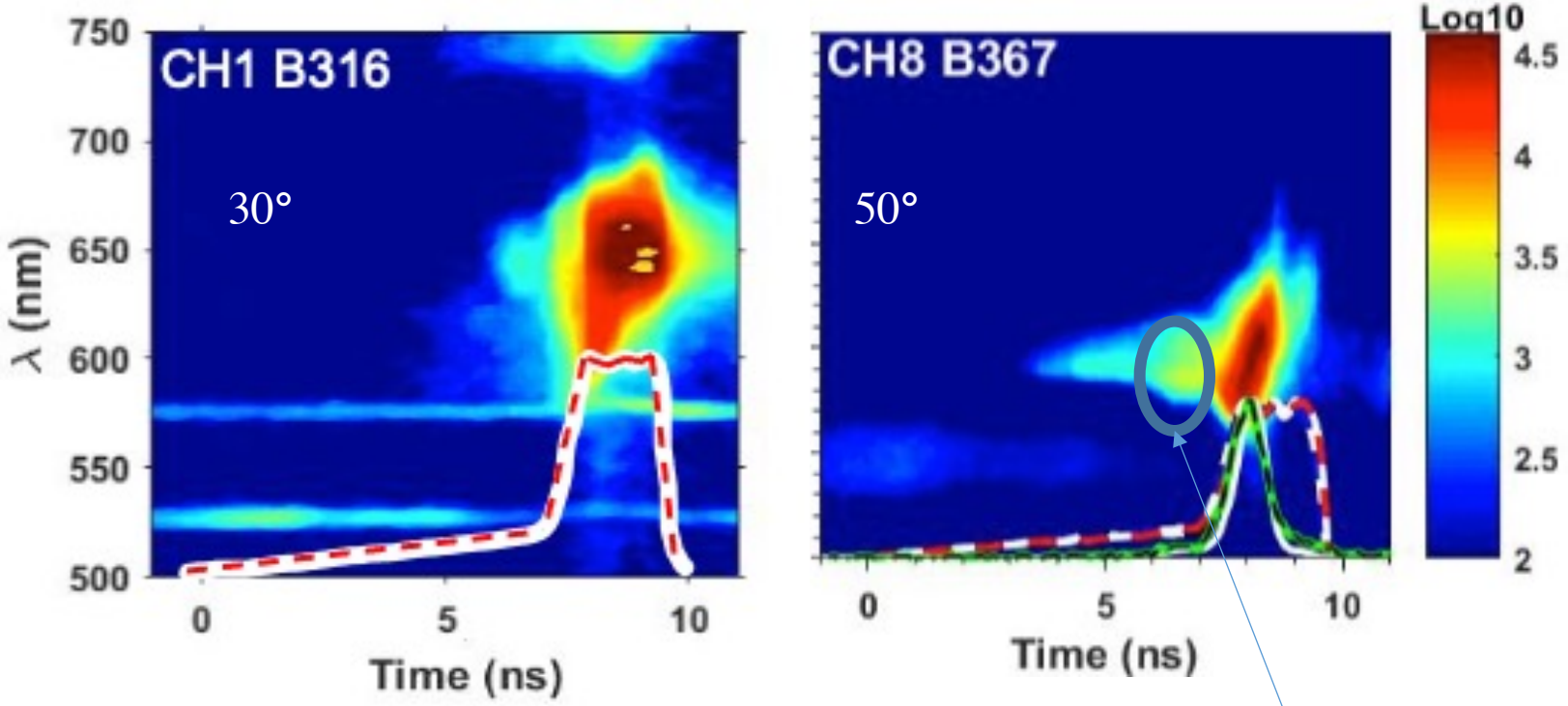

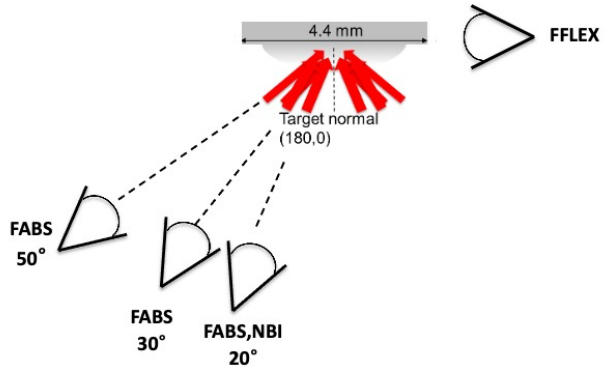

Side scattering

FABS suggests dependence of Raman emission on observation angle

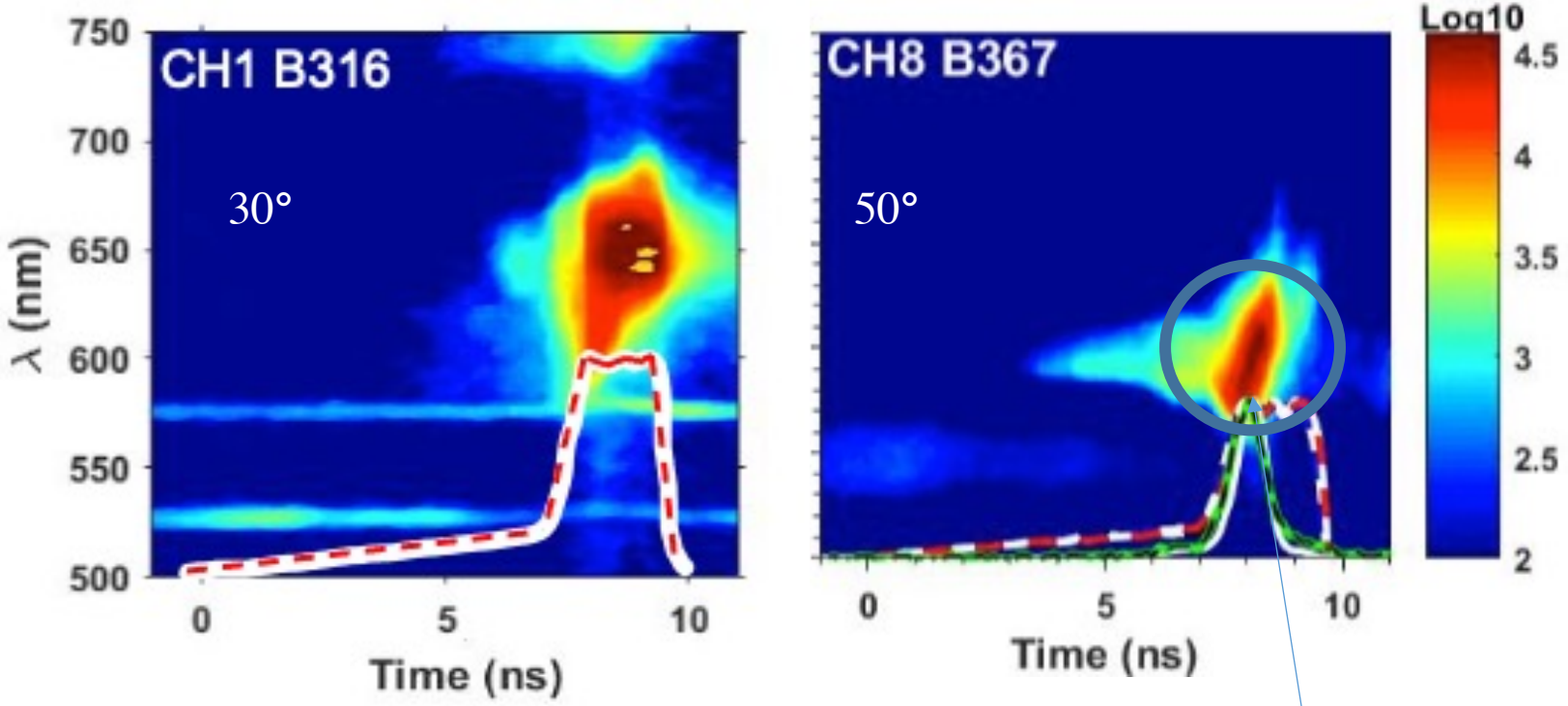

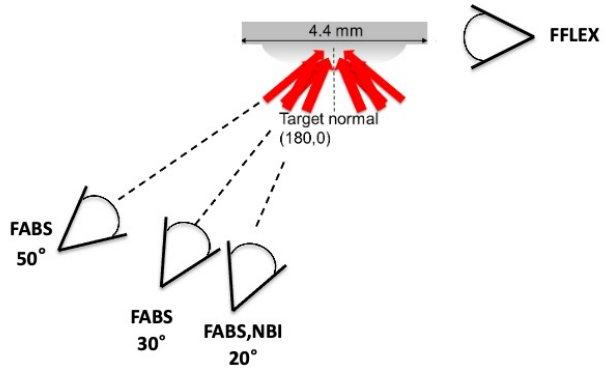

Back scattering?

FABS suggests dependence of Raman emission on observation angle

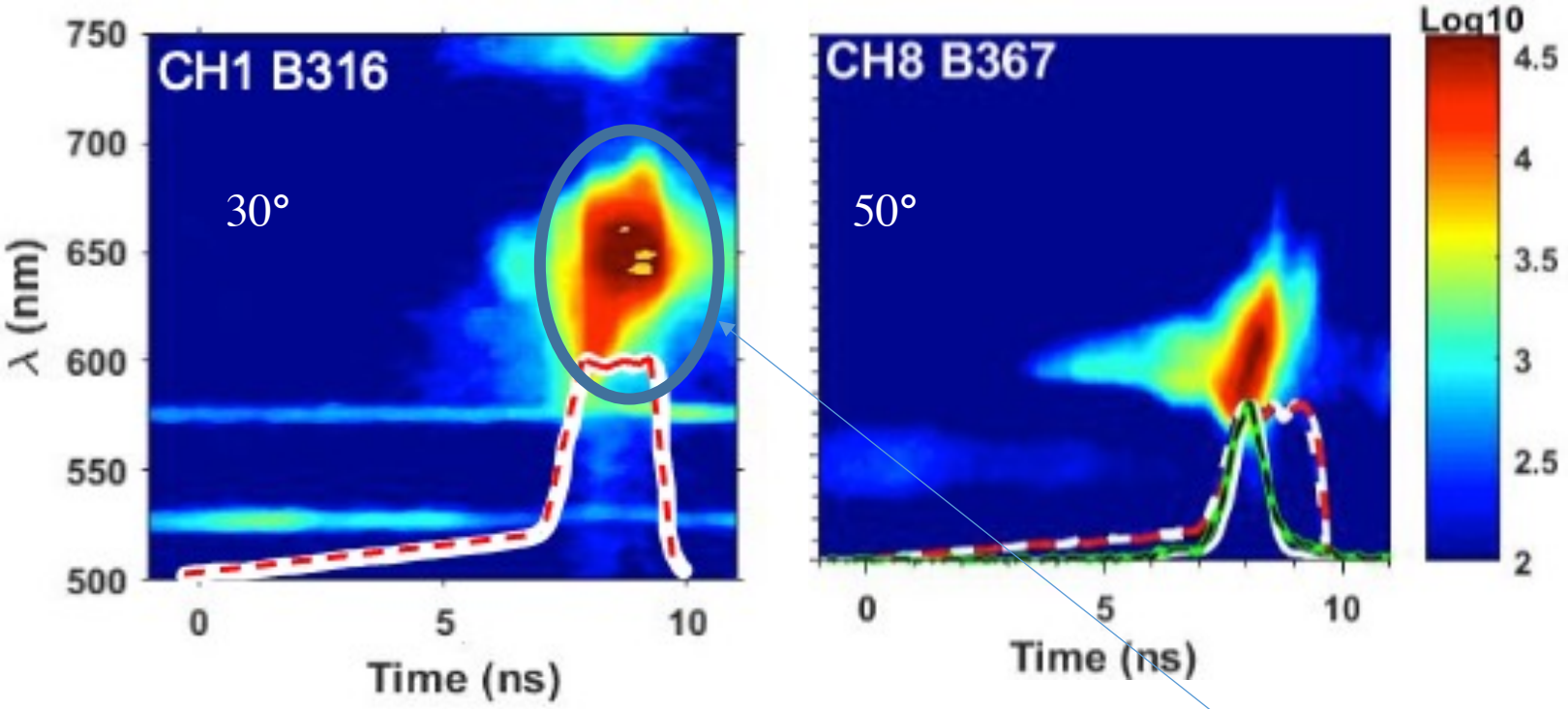

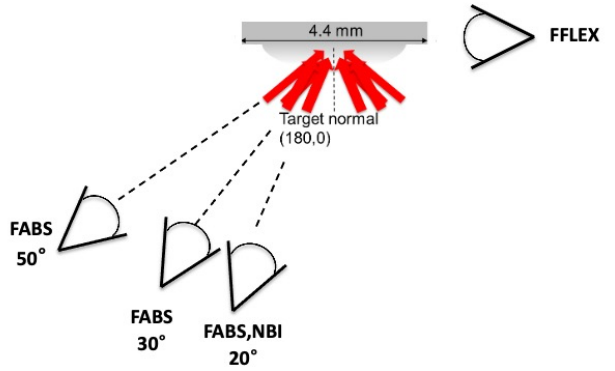

Back scattering

FABS suggests dependence of Raman emission on observation angle

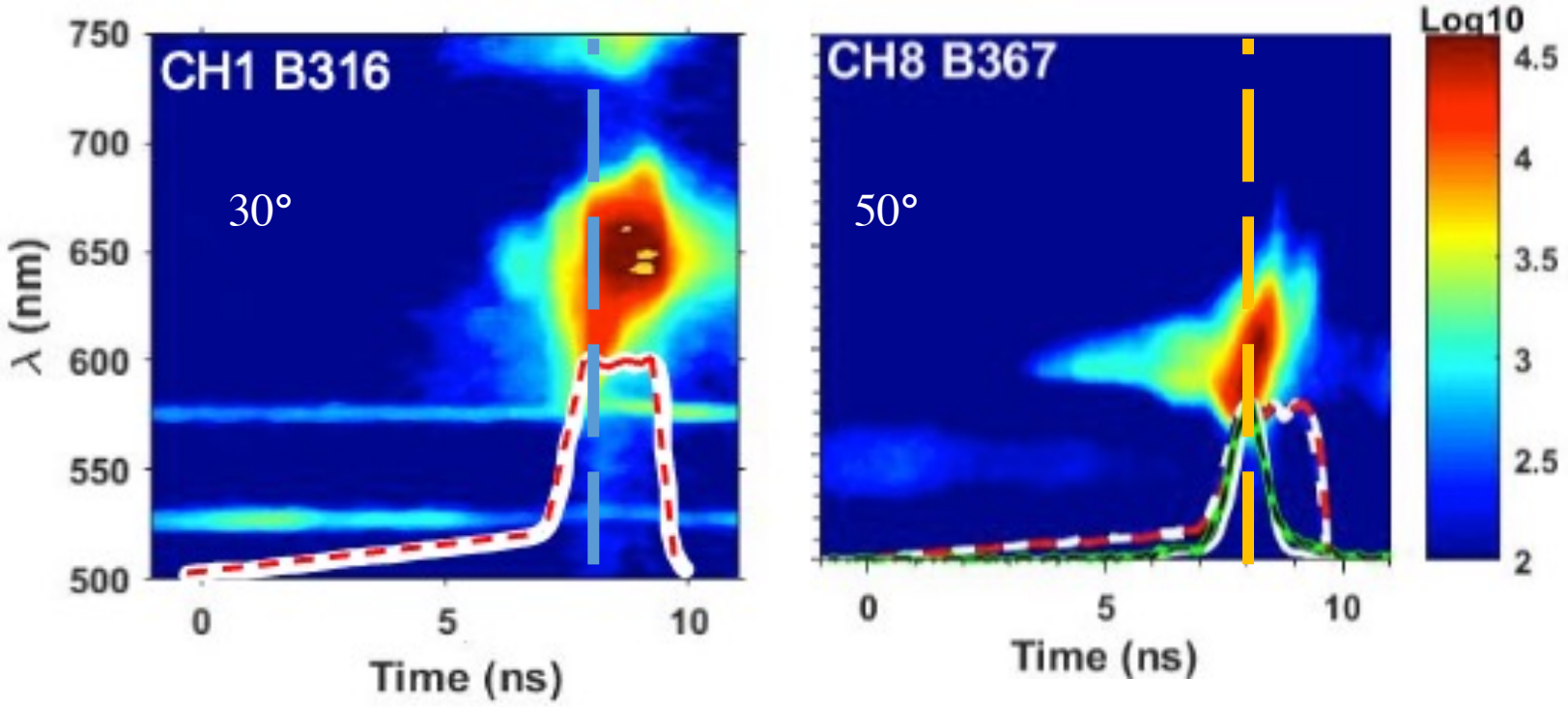

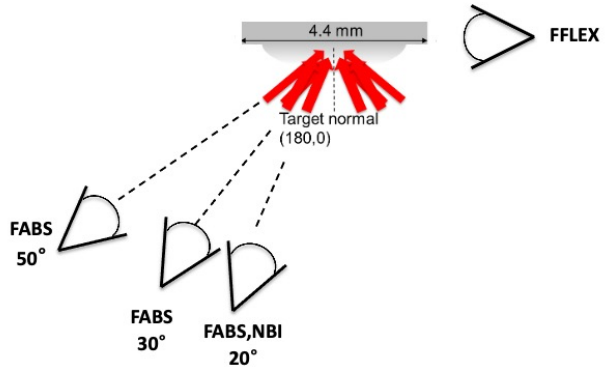

- Same amplitude as saturated

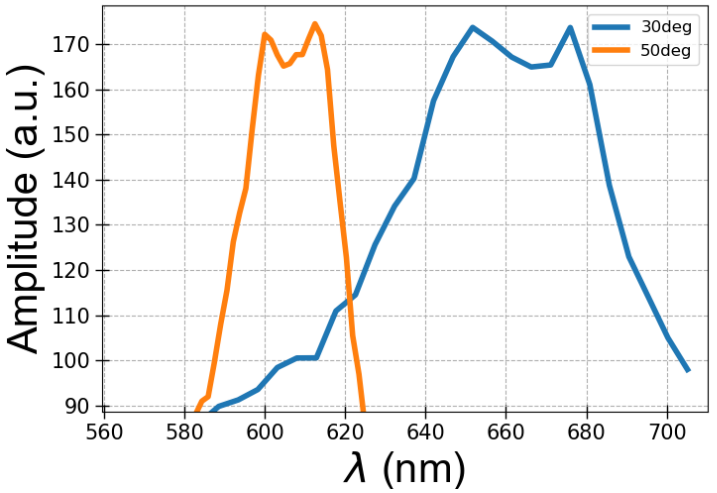

FABS suggests dependence of Raman emission on observation angle

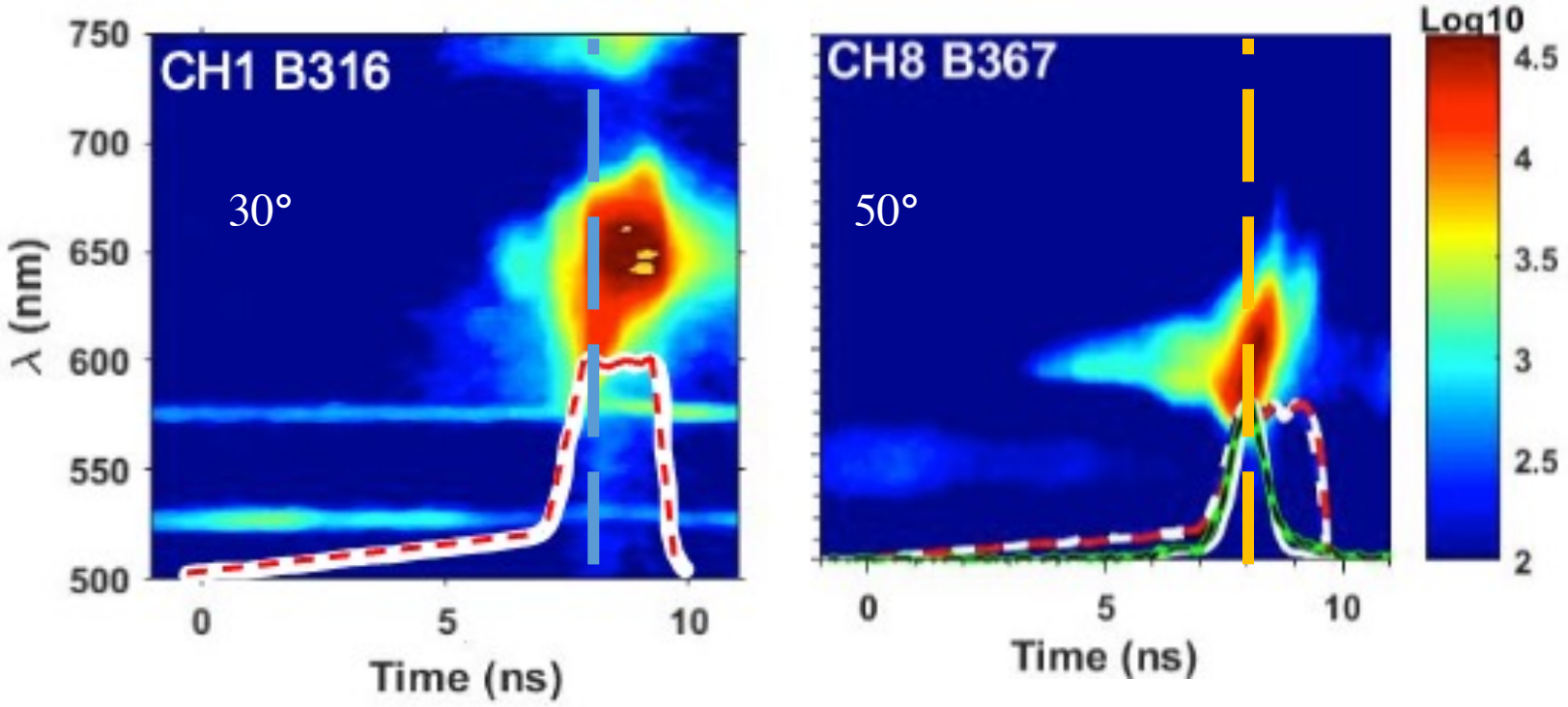

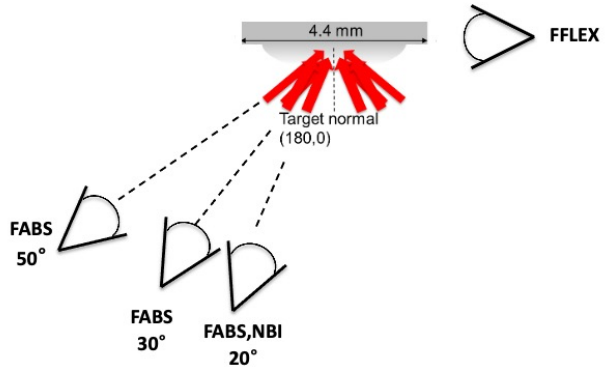

- Same amplitude as saturated
- Different upper wavelength cut-off -> 30deg signal broader

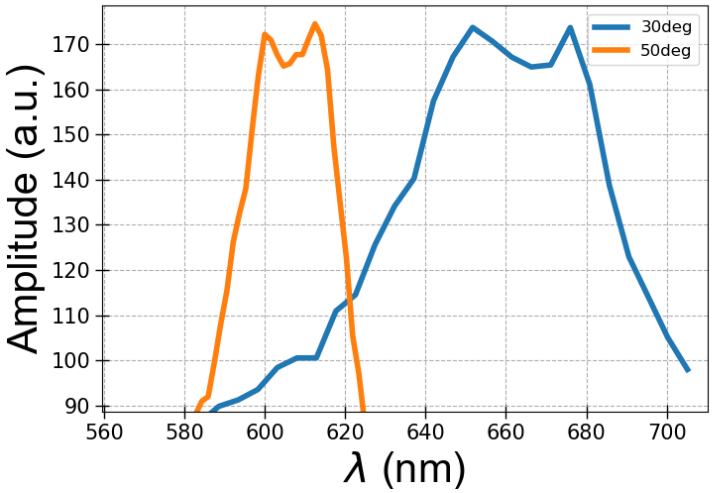

FABS suggests dependence of Raman emission on observation angle

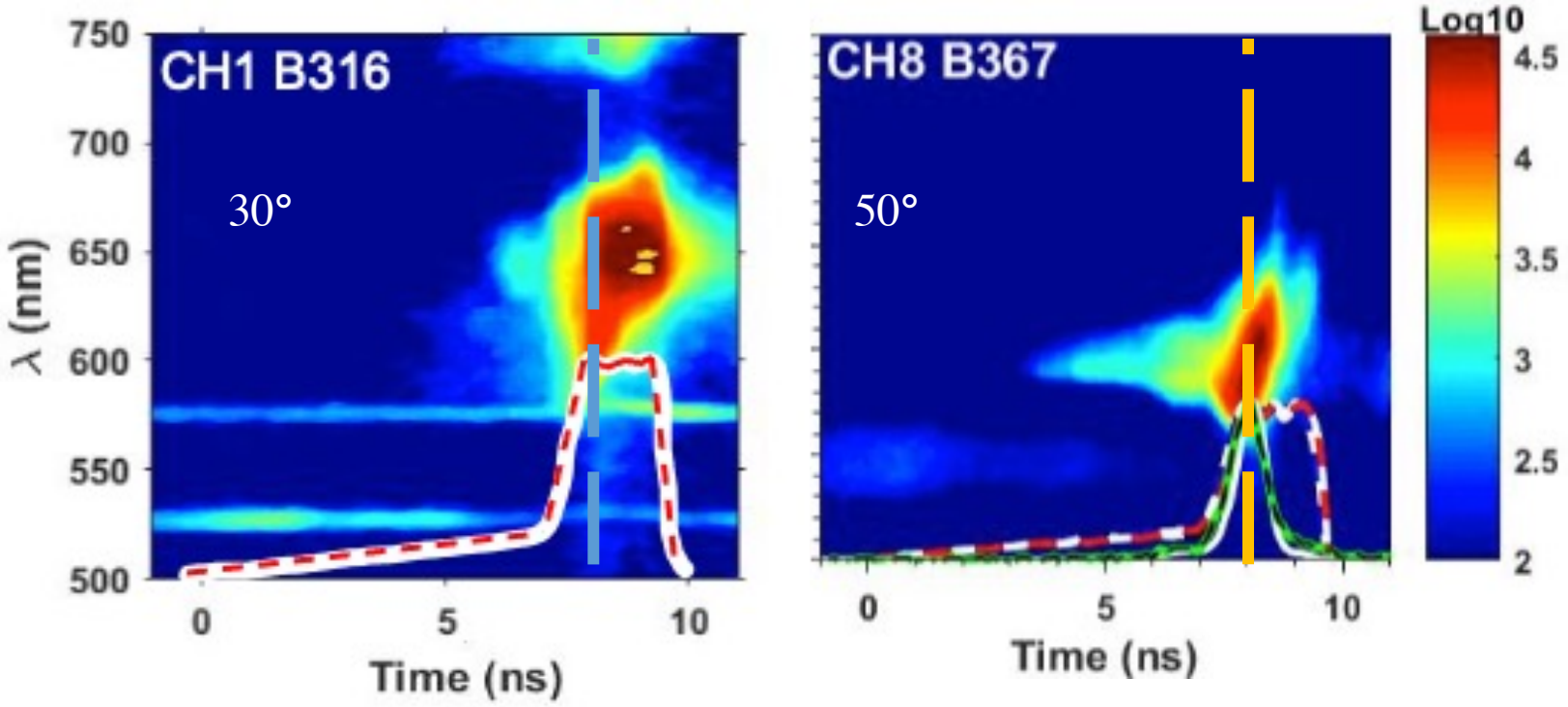

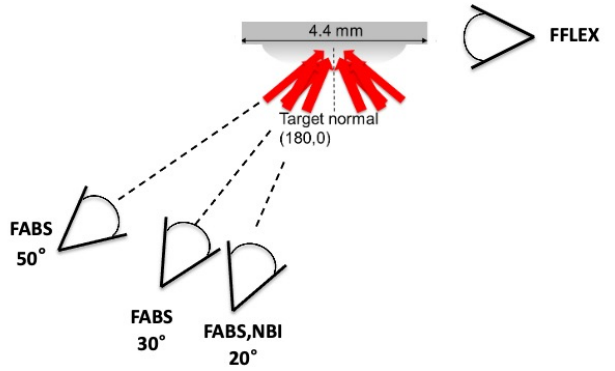

- Same amplitude as saturated
- Different upper wavelength cut-off -> 30deg signal broader

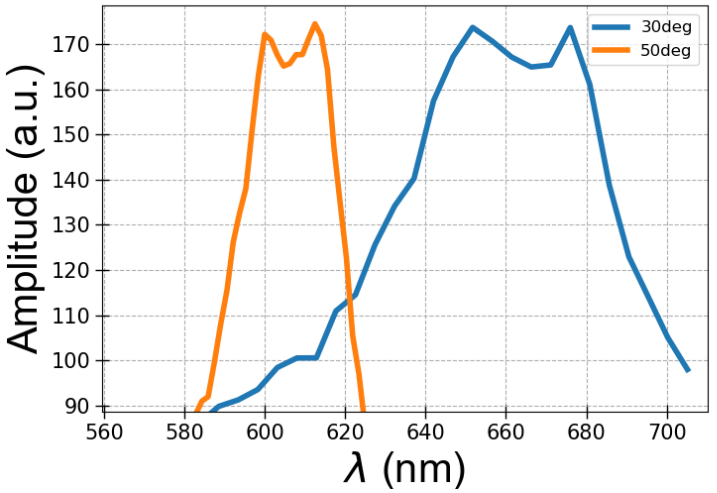

Is this difference a feature of Raman emission or another mechanism?

Raman refraction must be considered when comparing FABS signals

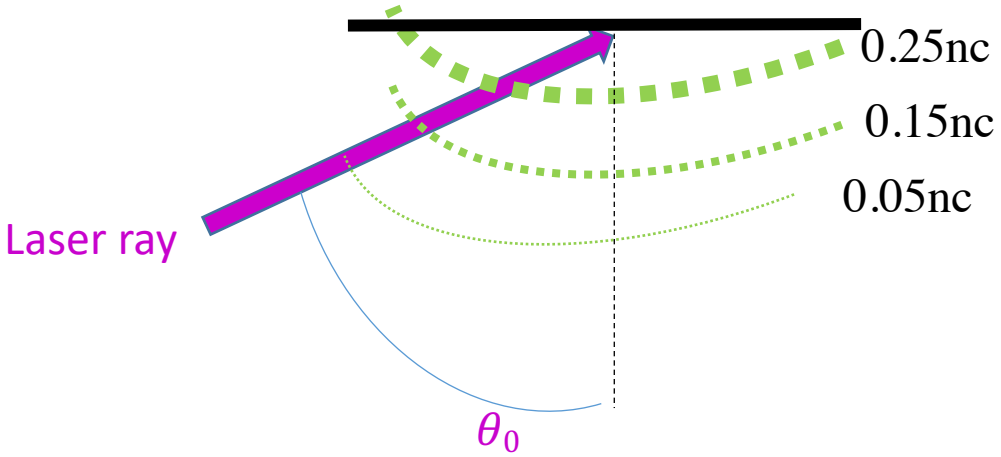

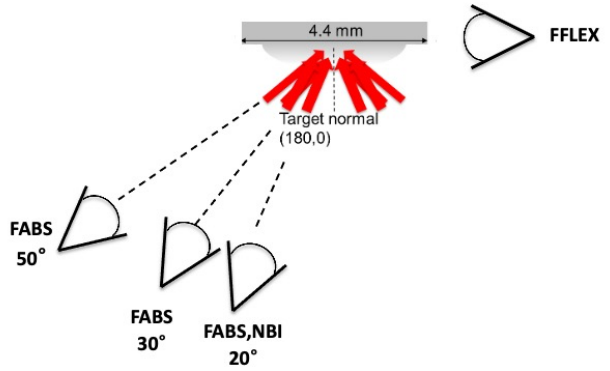

Raman refraction must be considered when comparing FABS signals

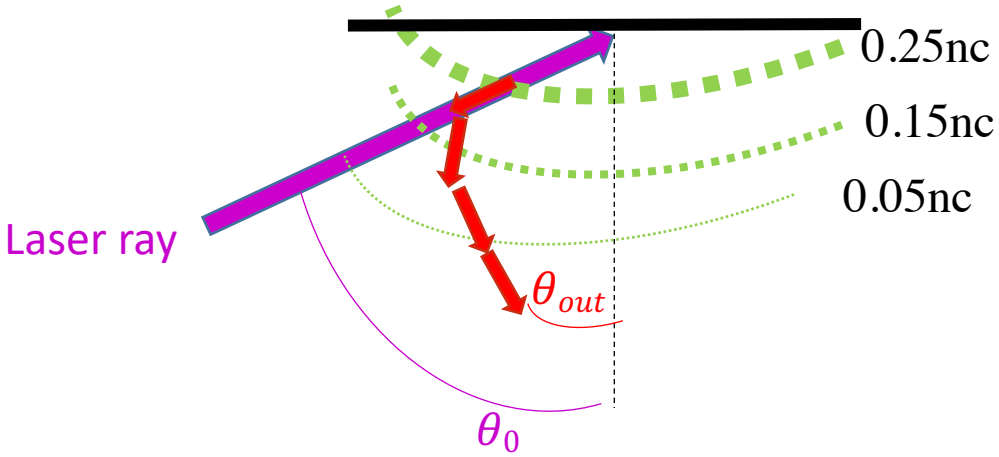

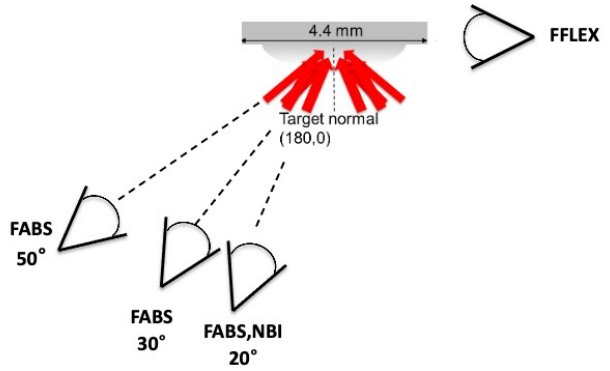

Raman refraction must be considered when comparing FABS signals

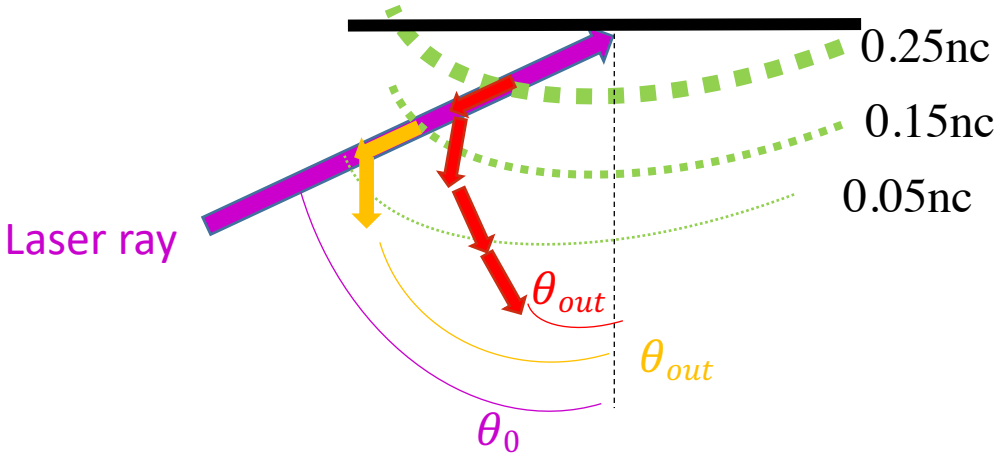

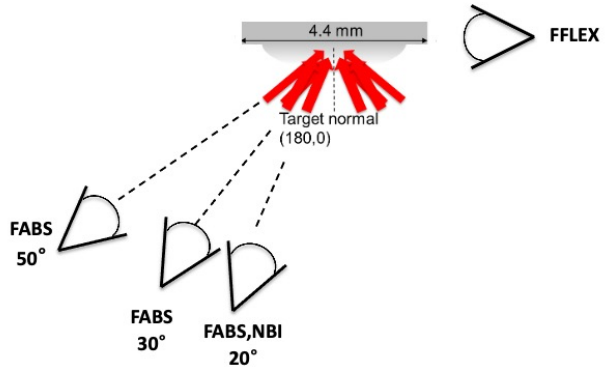

Raman refraction must be considered when comparing FABS signals

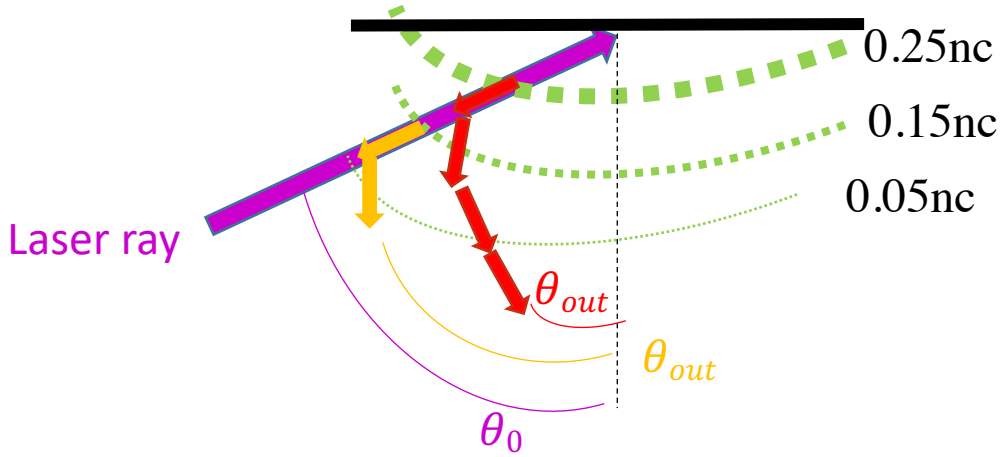

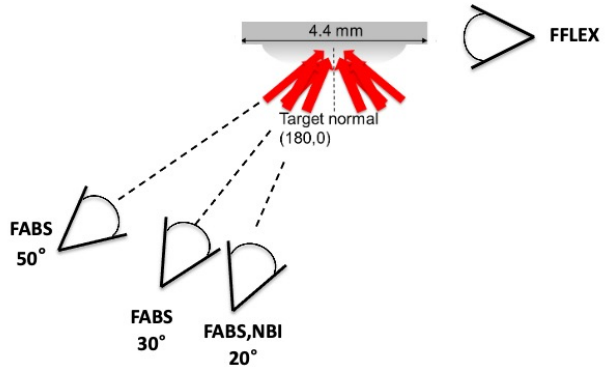

Snell's law

$$\sin(\theta_{\text{out}}) = \sin(\theta_0)\sqrt{\frac{1-\omega_{pr}^2/\omega_s^2}{1-\omega_{pr}^2/\omega_0^2}} \quad *$$

Raman refraction must be considered when comparing FABS signals

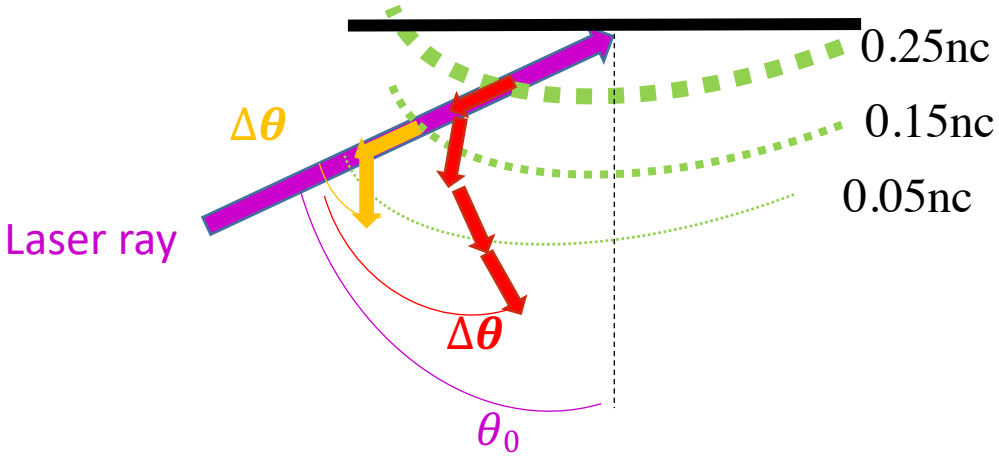

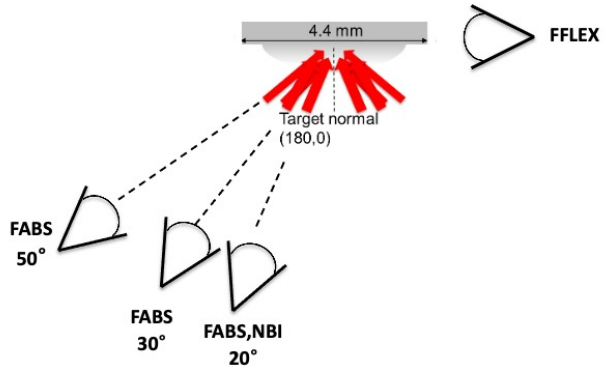

Snell's law

$$\sin(\theta_{\text{out}}) = \sin(\theta_0)\sqrt{\frac{1-\omega_{pr}^2/\omega_s^2}{1-\omega_{pr}^2/\omega_0^2}} \quad *$$

$$\Delta\theta = \theta_{\text{out}} - \theta_0$$

Exit angle of Raman ray relative to incident light ray

*Michel, PRE **99**, 033203 (2019)

Raman refraction must be considered when comparing FABS signals

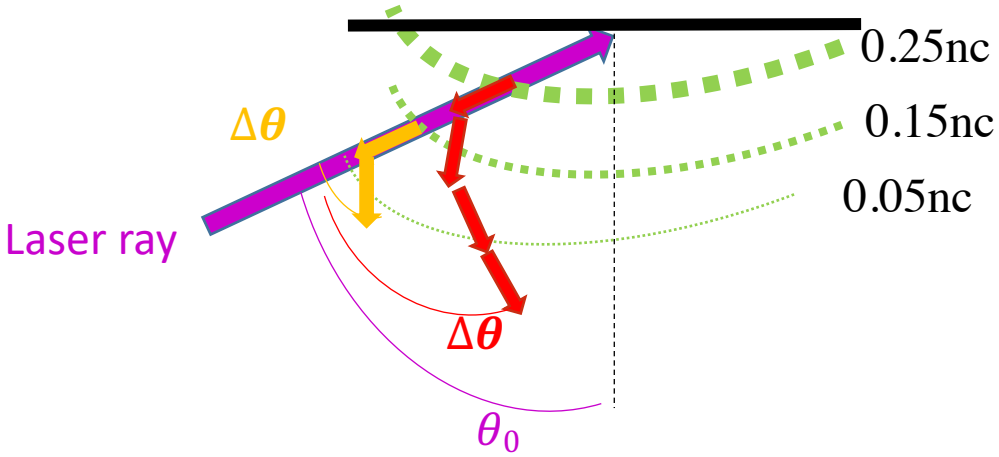

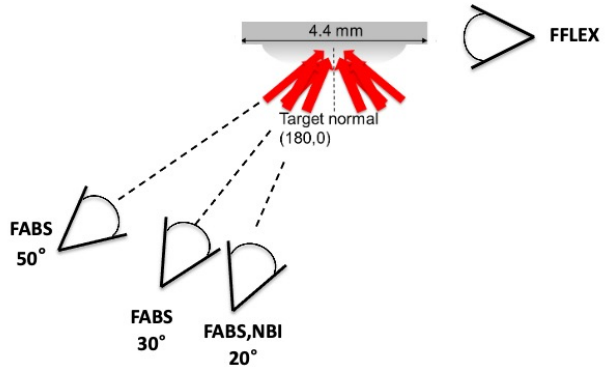

Snell's law

$$\sin(\theta_{\text{out}}) = \sin(\theta_0)\sqrt{\frac{1-\omega_{pr}^2/\omega_s^2}{1-\omega_{pr}^2/\omega_0^2}} \quad *$$

$$\Delta\theta = \theta_{\text{out}} - \theta_0$$

Exit angle of Raman ray relative to incident light ray

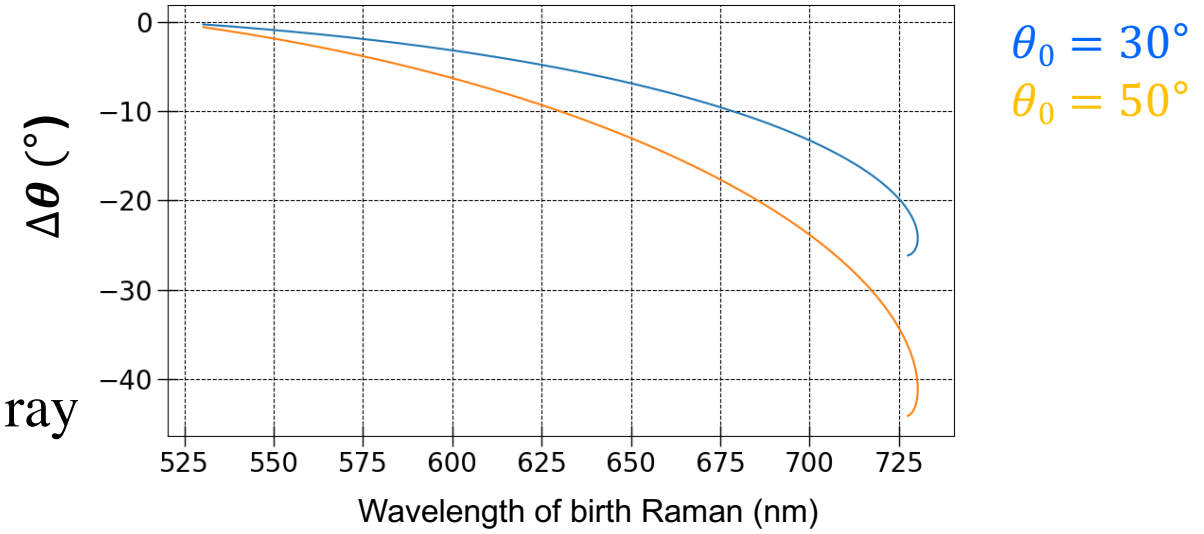

*Michel, PRE **99**, 033203 (2019)

Raman refraction must be considered when comparing FABS signals

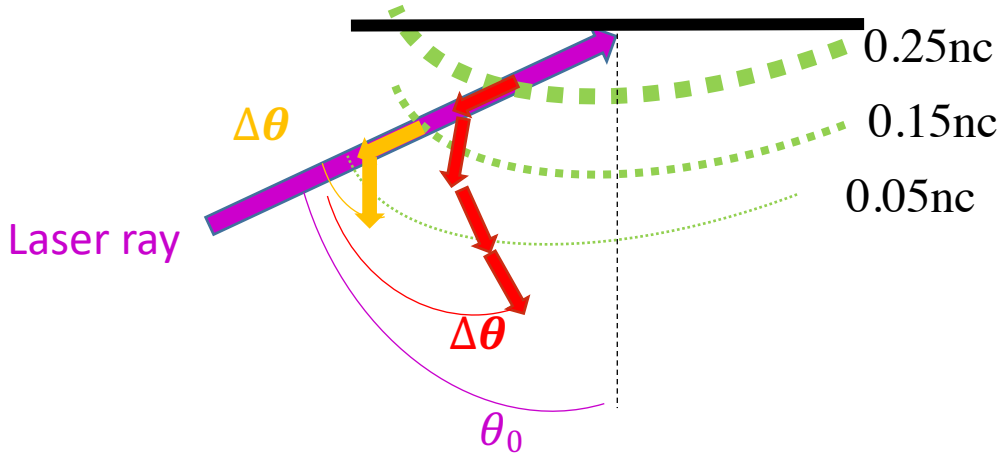

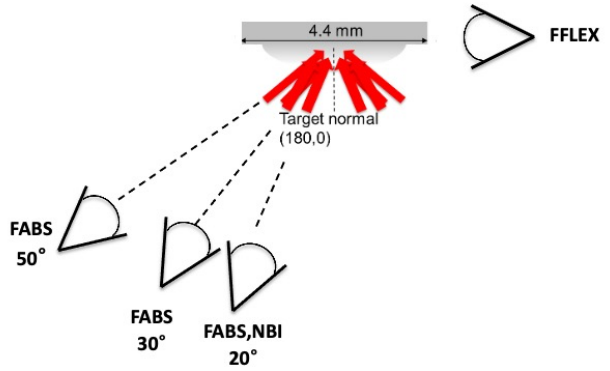

Snell's law

$$\sin(\theta_{\text{out}}) = \sin(\theta_0)\sqrt{\frac{1-\omega_{pr}^2/\omega_s^2}{1-\omega_{pr}^2/\omega_0^2}} \quad *$$

$$\Delta\theta = \theta_{\text{out}} - \theta_0$$

Exit angle of Raman ray relative to incident light ray

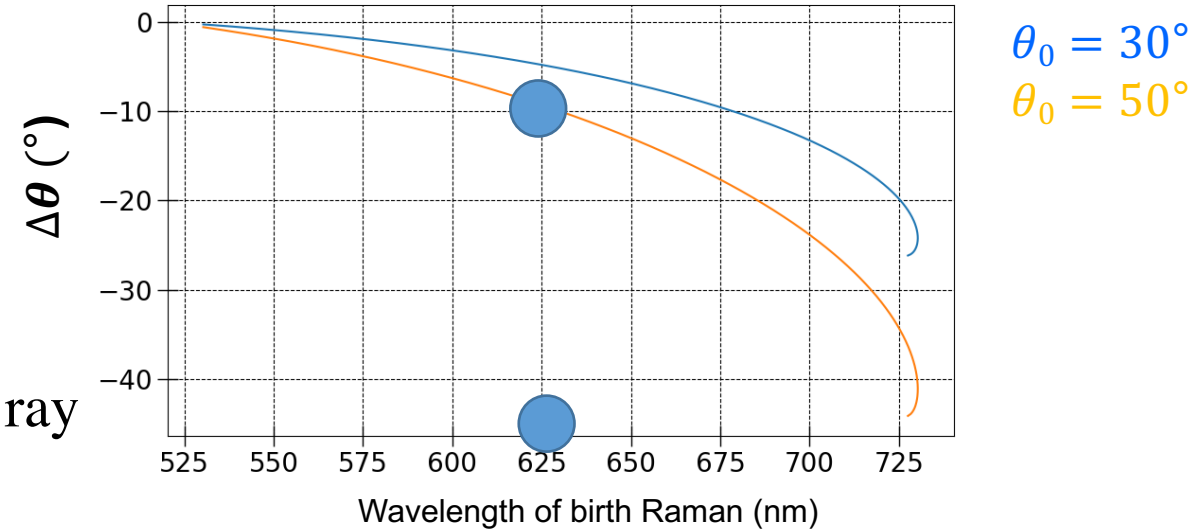

*Michel, PRE **99**, 033203 (2019)

Raman refraction must be considered when comparing FABS signals

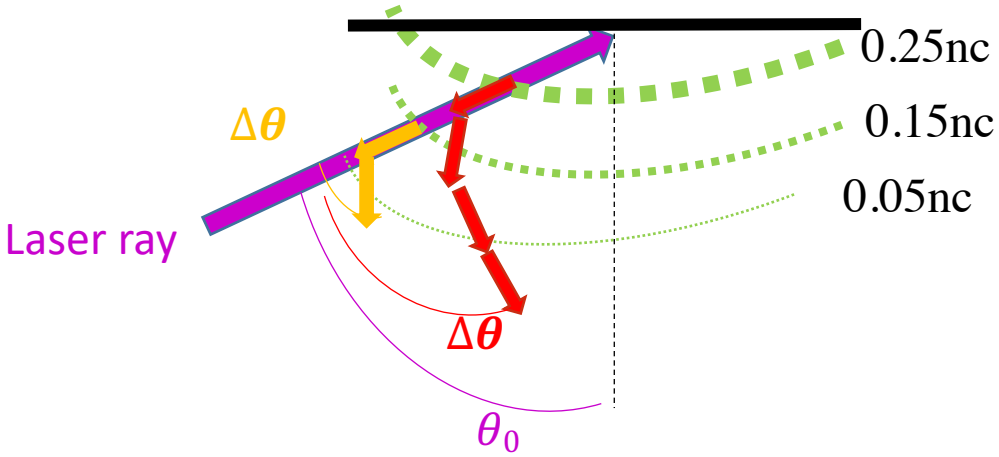

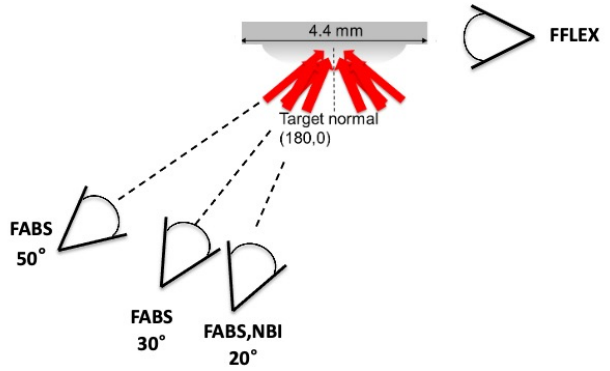

Snell's law

$$\sin(\theta_{\text{out}}) = \sin(\theta_0)\sqrt{\frac{1-\omega_{pr}^2/\omega_s^2}{1-\omega_{pr}^2/\omega_0^2}} \quad *$$

$$\Delta\theta = \theta_{\text{out}} - \theta_0$$

Exit angle of Raman ray relative to incident light ray

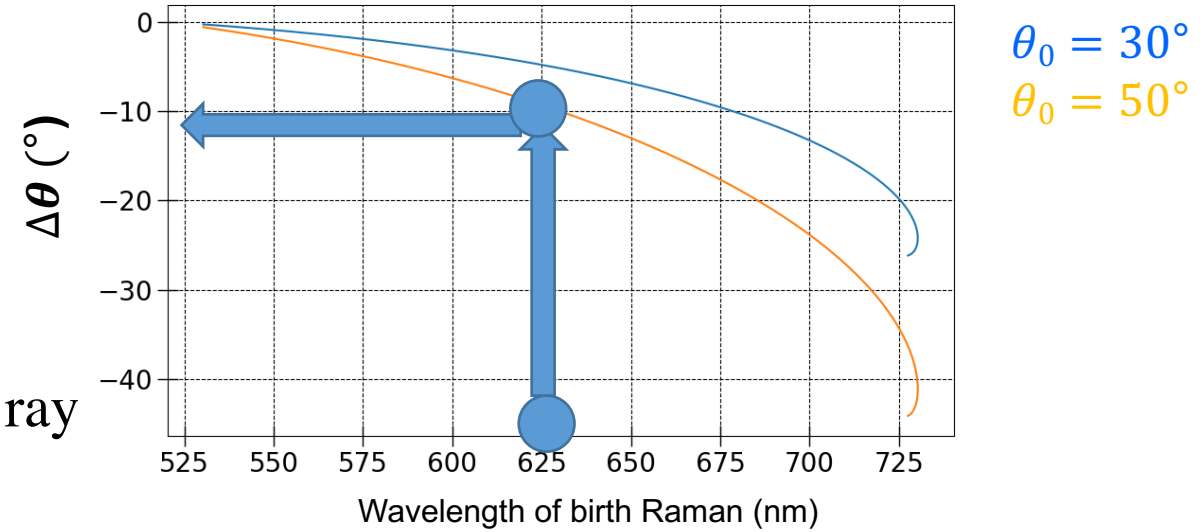

*Michel, PRE **99**, 033203 (2019)

Which refracted Raman rays enter FABS?

Snell's law

$$\sin(\theta_{out}) = \sin(\theta_0)\sqrt{\frac{1-\omega_{pr}^2/\omega_s^2}{1-\omega_{pr}^2/\omega_0^2}}$$

$$\Delta\theta = \theta_{out} - \theta_0$$

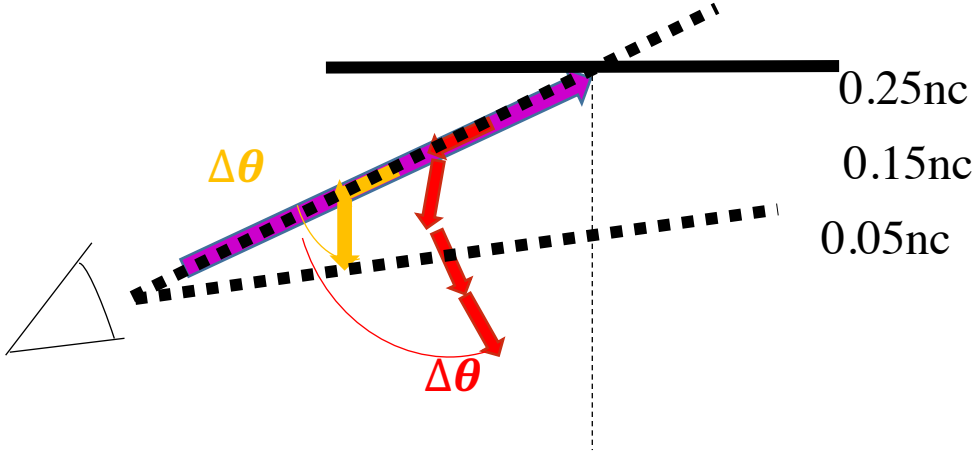

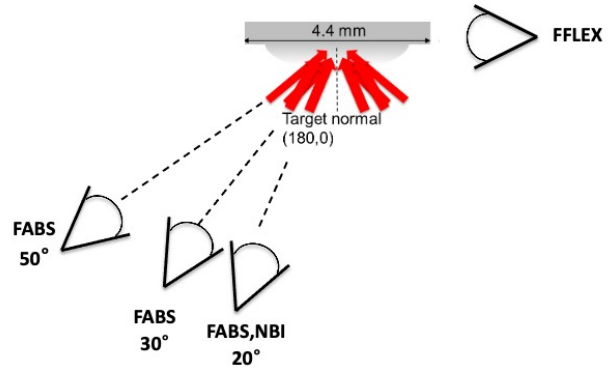

Range of Fabs collection angle

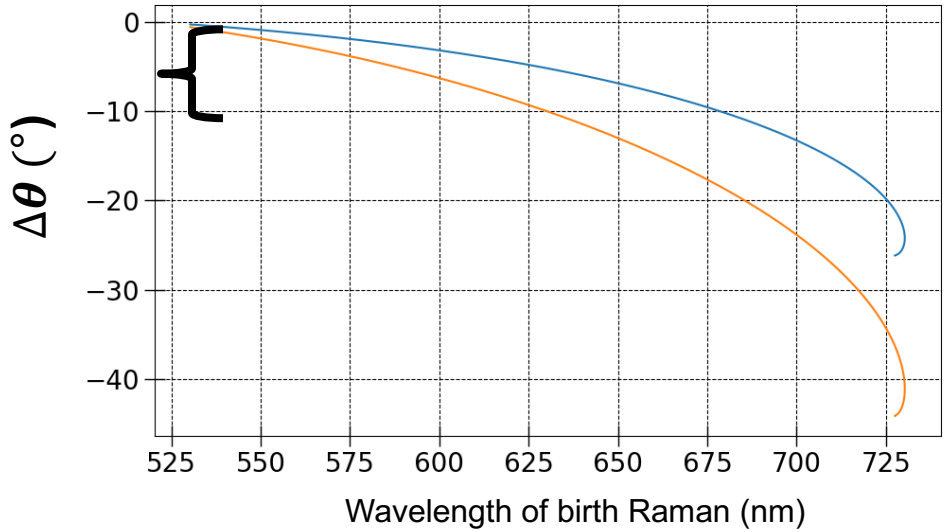

$\theta_0 = 30°$

$\theta_0 = 50°$

Which refracted Raman rays enter FABS?

Snell's law

$$\sin(\theta_{\text{out}}) = \sin(\theta_0)\sqrt{\frac{1-\omega_{pr}^2/\omega_s^2}{1-\omega_{pr}^2/\omega_0^2}}$$

$$\Delta\theta = \theta_{\text{out}} - \theta_0$$

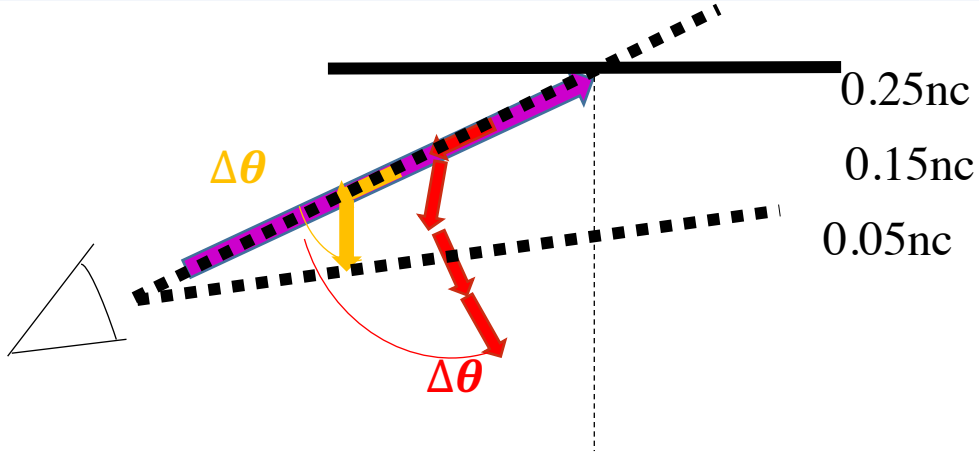

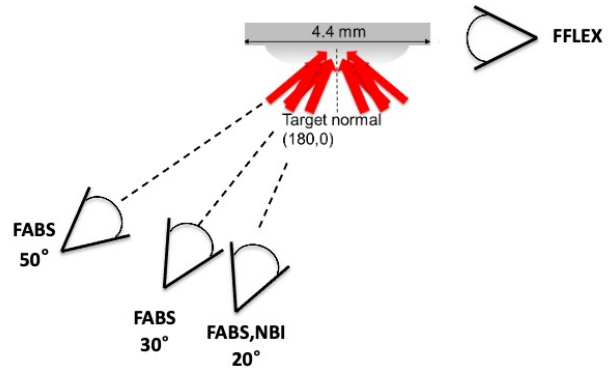

Range of Fabs collection angle

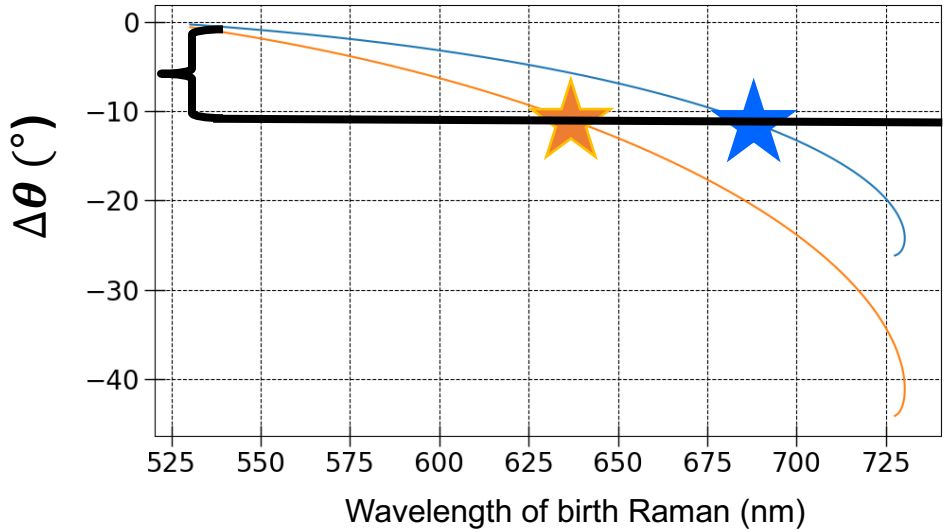

$\theta_0 = 30°$

$\theta_0 = 50°$

Which refracted Raman rays enter FABS?

Snell's law

$$\sin(\theta_{out}) = \sin(\theta_0)\sqrt{\frac{1-\omega_{pr}^2/\omega_s^2}{1-\omega_{pr}^2/\omega_0^2}}$$

$$\Delta\theta = \theta_{out} - \theta_0$$

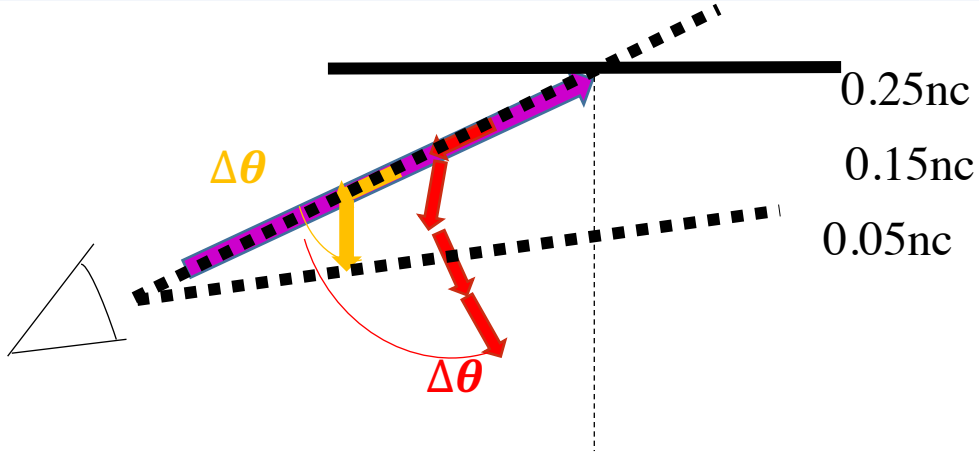

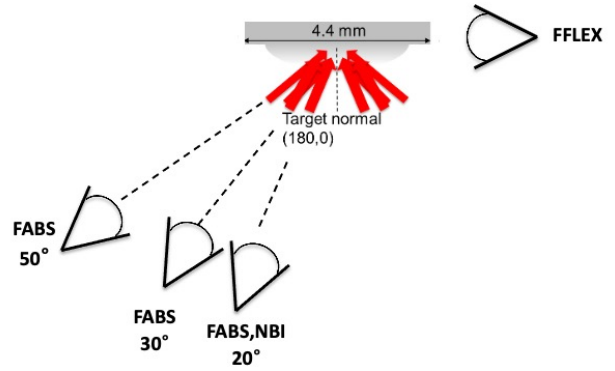

Range of Fabs collection angle

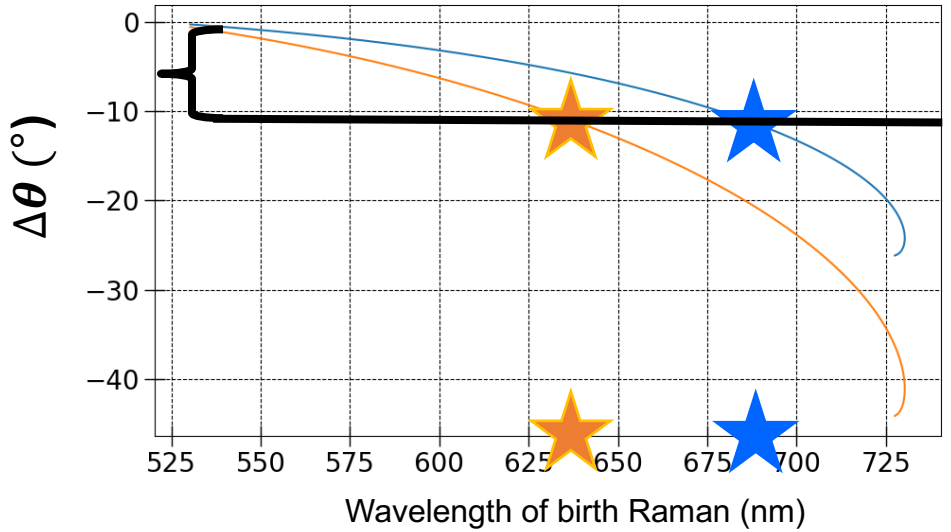

$\theta_0 = 30°$

$\theta_0 = 50°$

Which refracted Raman rays enter FABS?

Snell's law

$$\sin(\theta_{out}) = \sin(\theta_0)\sqrt{\frac{1-\omega_{pr}^2/\omega_s^2}{1-\omega_{pr}^2/\omega_0^2}}$$

$$\Delta\theta = \theta_{out} - \theta_0$$

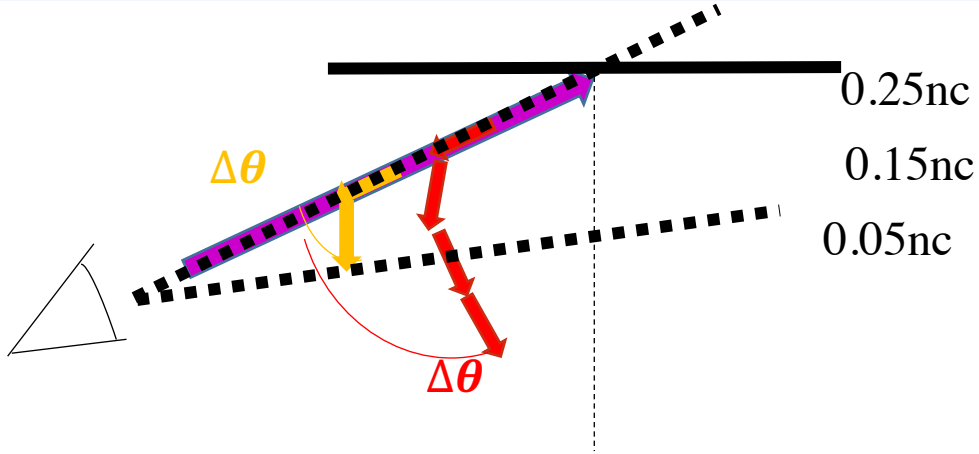

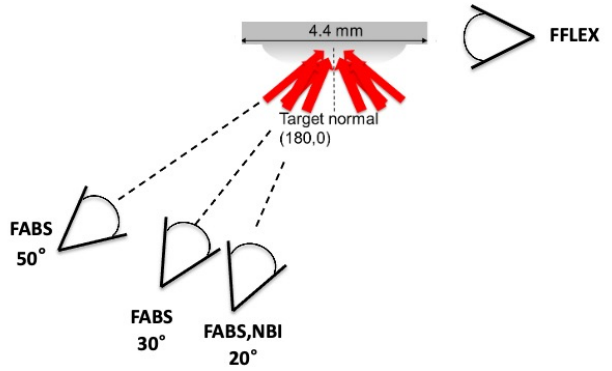

Upper wavelength cut-off

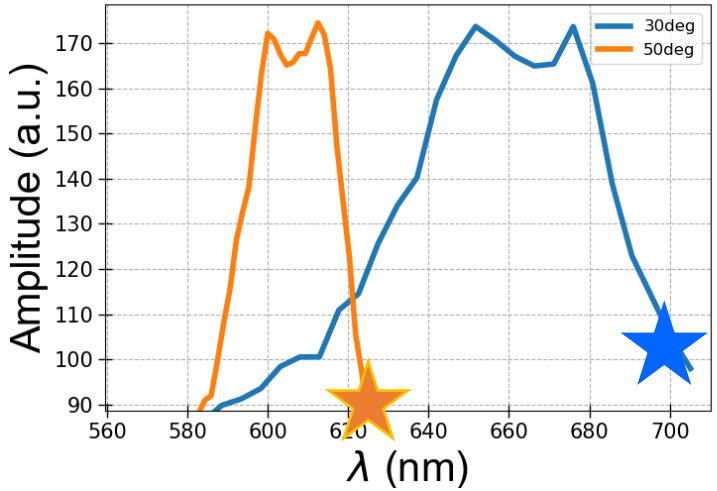

Range of Fabs collection angle

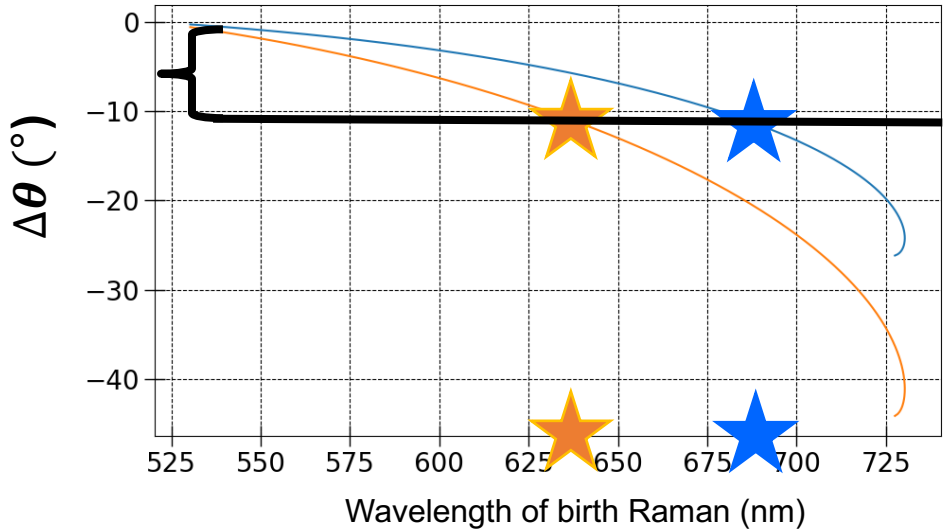

$\theta_0 = 30°$

$\theta_0 = 50°$

NBI plate image indicates Raman light only partially enters FABS

Time-integrated Raman light (400-700 nm)

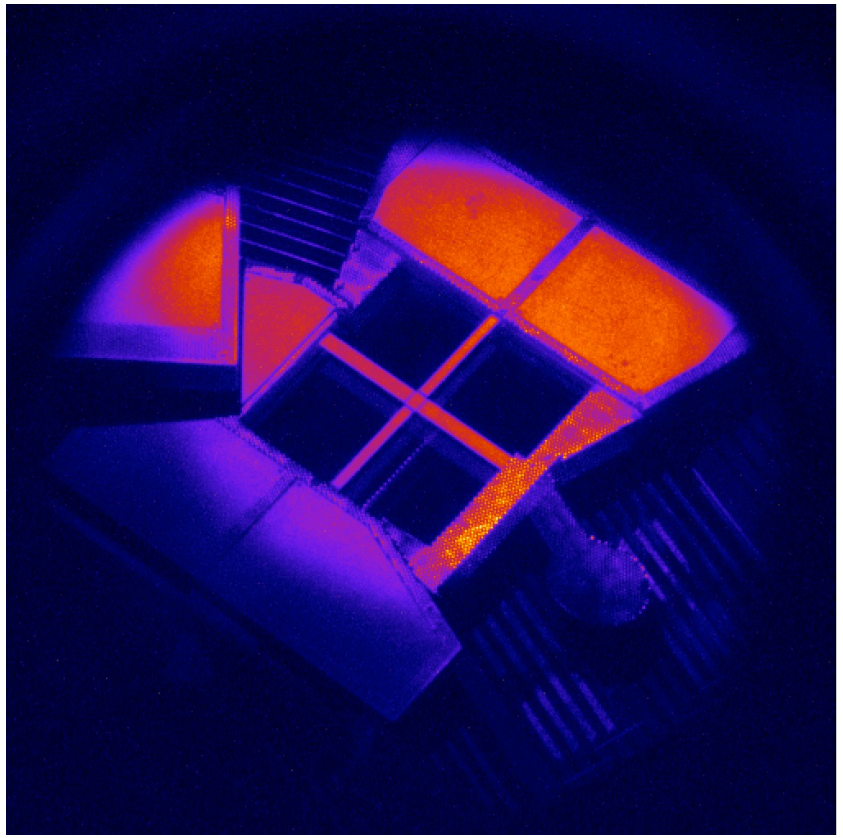

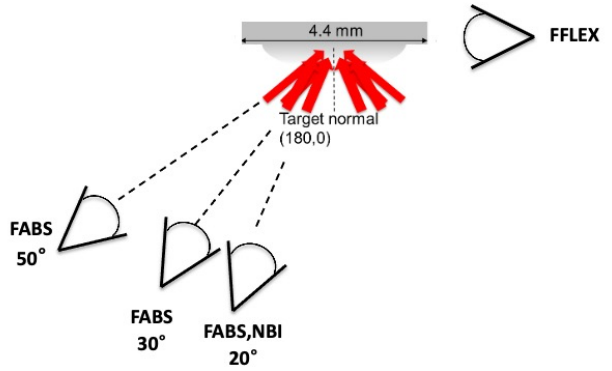

NBI plate image indicates Raman light only partially enters FABS

Time-integrated Raman light (400-700 nm)

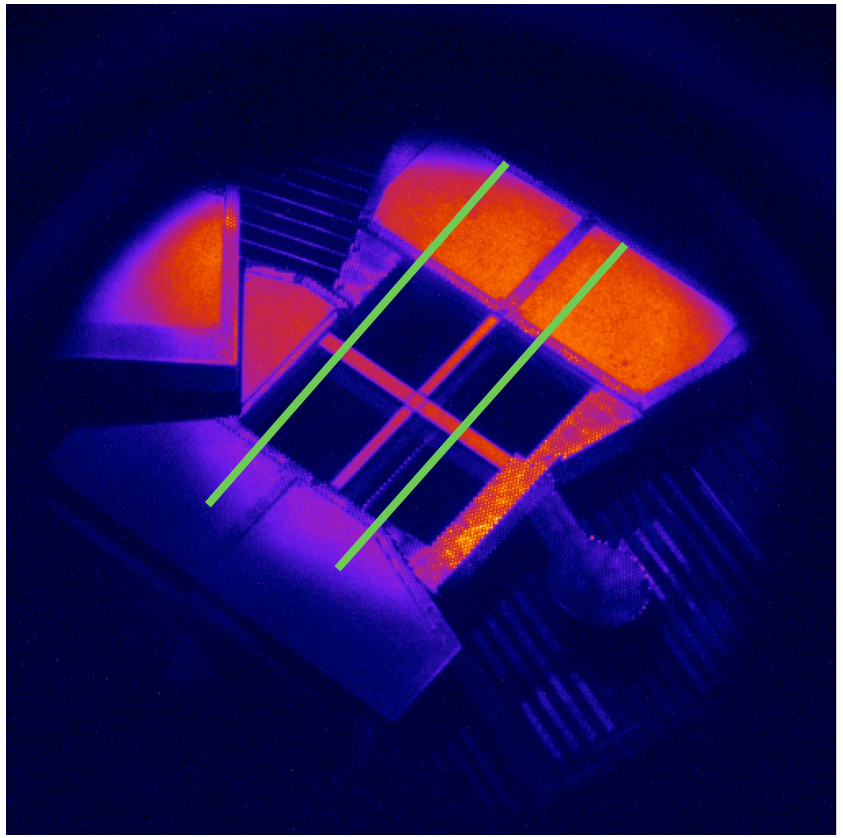

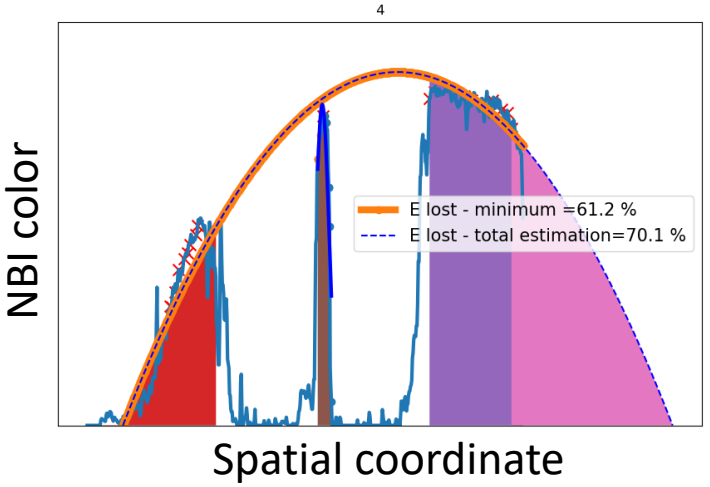

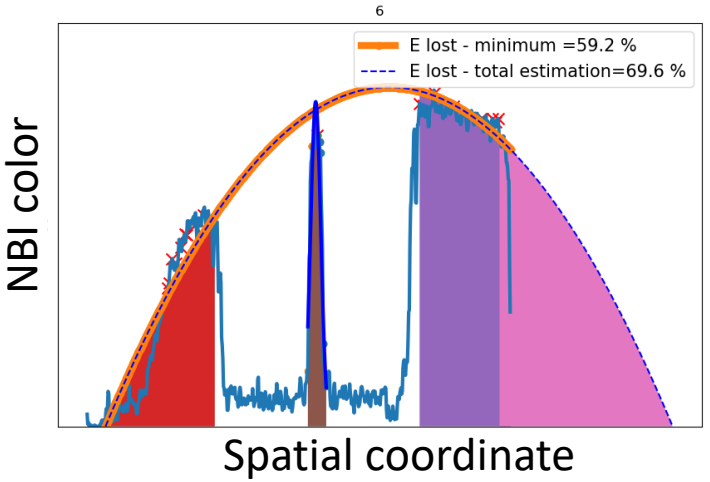

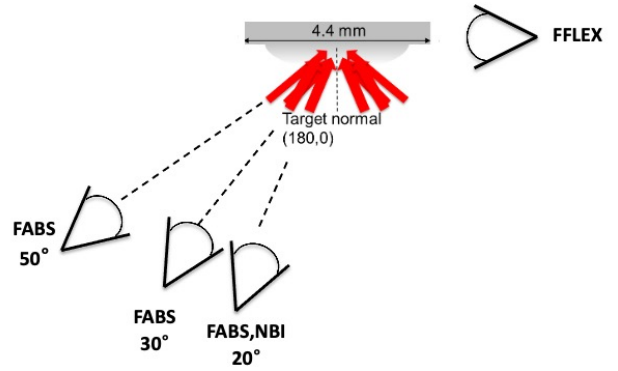

Approximately 60%-70% of Raman light is not detected; 2.5% corrected reflectivity

Numerical modelling (preliminary)

Hydrodynamics simulations gave underdense plasma conditions for PIC simulations

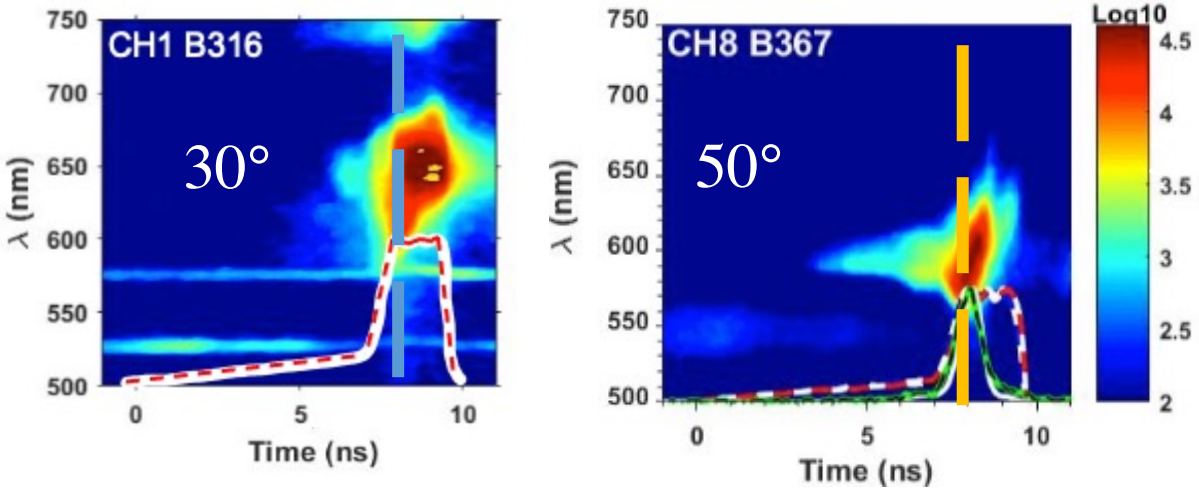

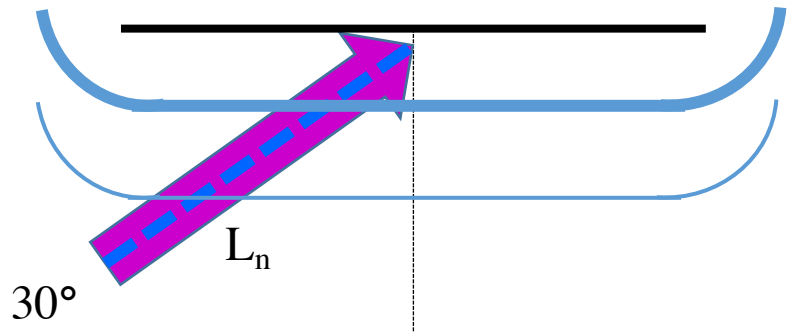

deg	t (ns)	L_n (um)	T_e (nc/4) (keV)	T_i (nc/4) (kev)	I_0 (10^{16} W/cm^2)	V(ne=0.1nc) (1e6 m/s)	V(ne=0.25nc) (1e6 m/s)
30	8	720	7.5	1.5	1	-0.9	-0.55
50	8	600	7	1.5	1	-0.3	-0.1

Hydrodynamics simulations gave underdense plasma conditions for PIC simulations

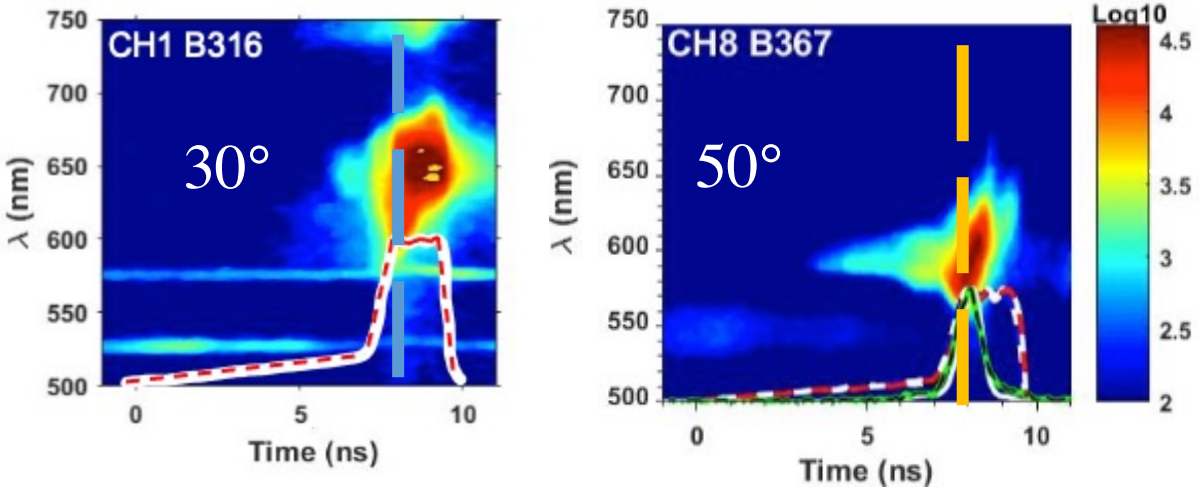

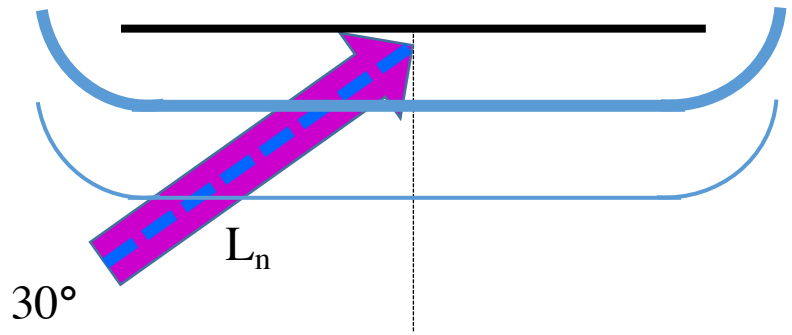

deg	t (ns)	L_n (um)	T_e (nc/4) (keV)	T_i (nc/4) (kev)	I_0 (10^{16} W/cm^2)	V(ne=0.1nc) (1e6 m/s)	V(ne=0.25nc) (1e6 m/s)
30	8	720	7.5	1.5	1	-0.9	-0.55
50	8	600	7	1.5	1	-0.3	-0.1

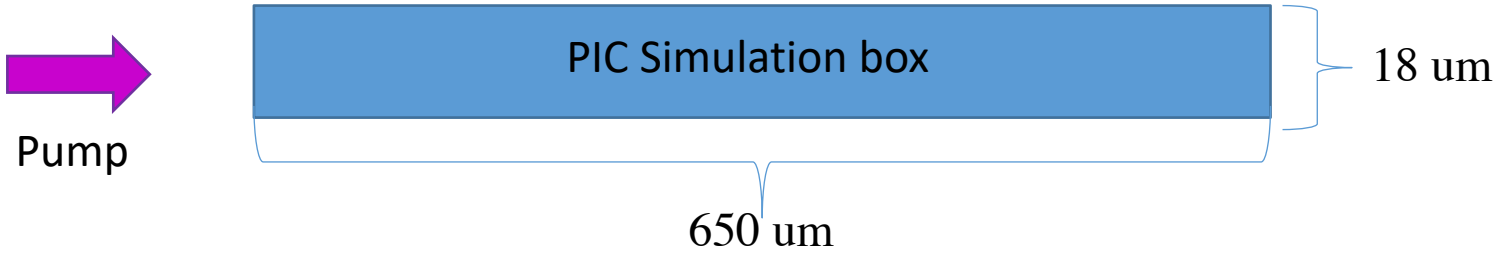

Simulations also indicate wavelength shift is due to Raman refraction

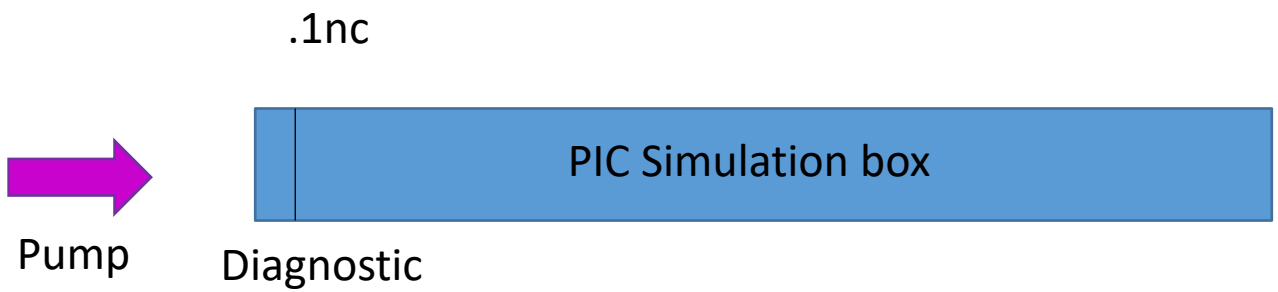

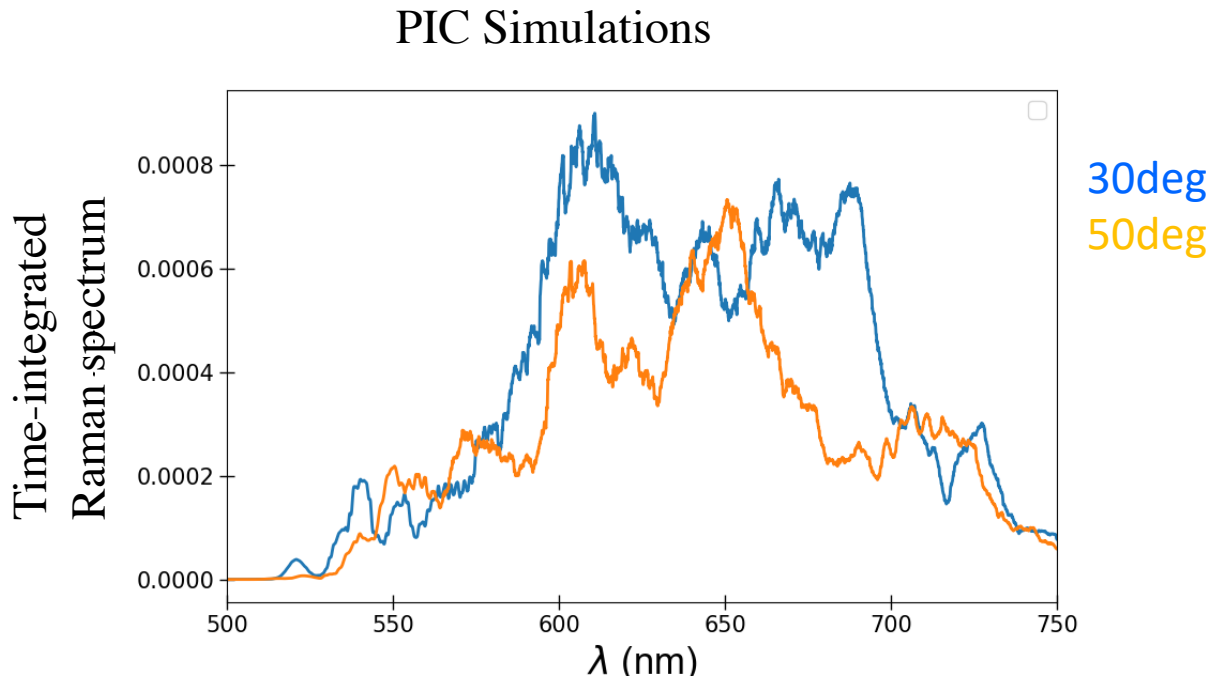

Simulations also indicate wavelength shift is due to Raman refraction

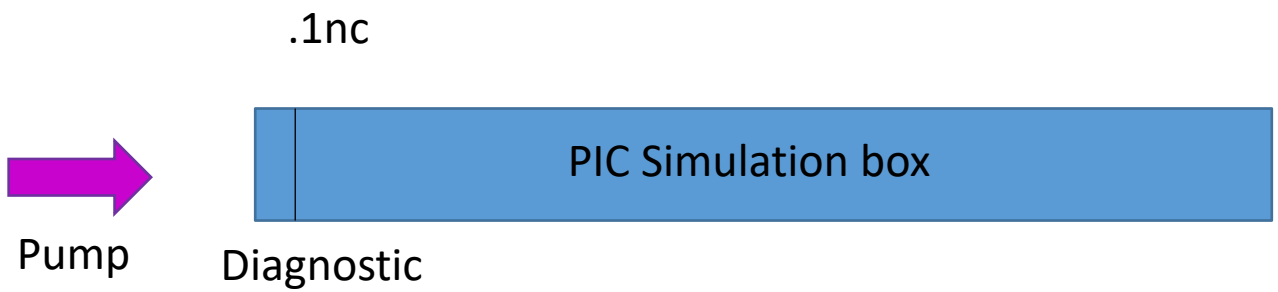

FABS data: clear shift

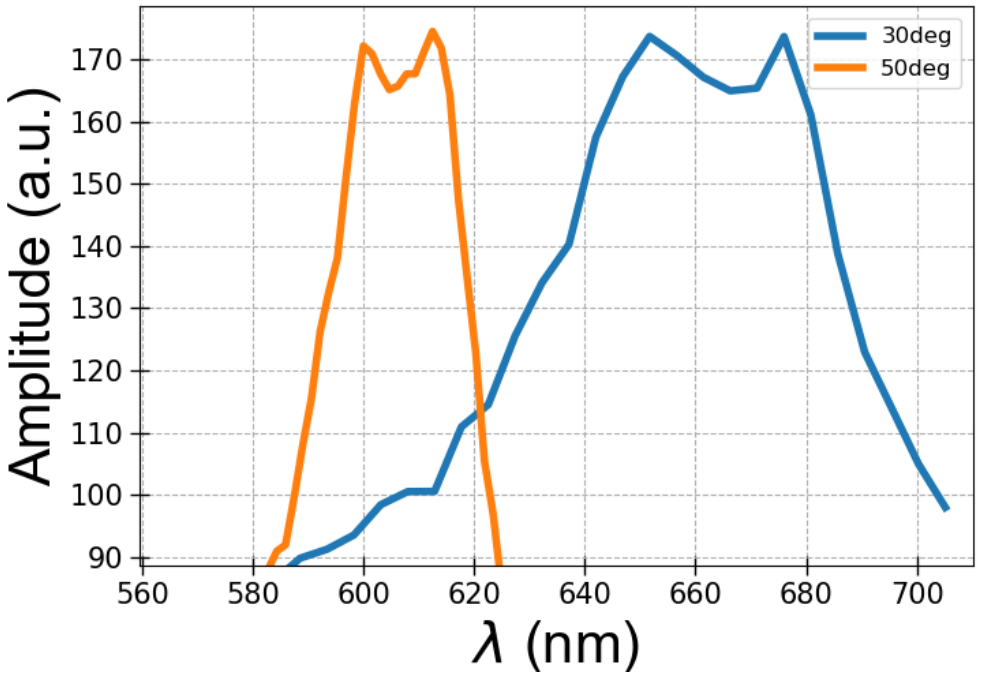

PIC Simulations: no clear shift (refraction not captured)

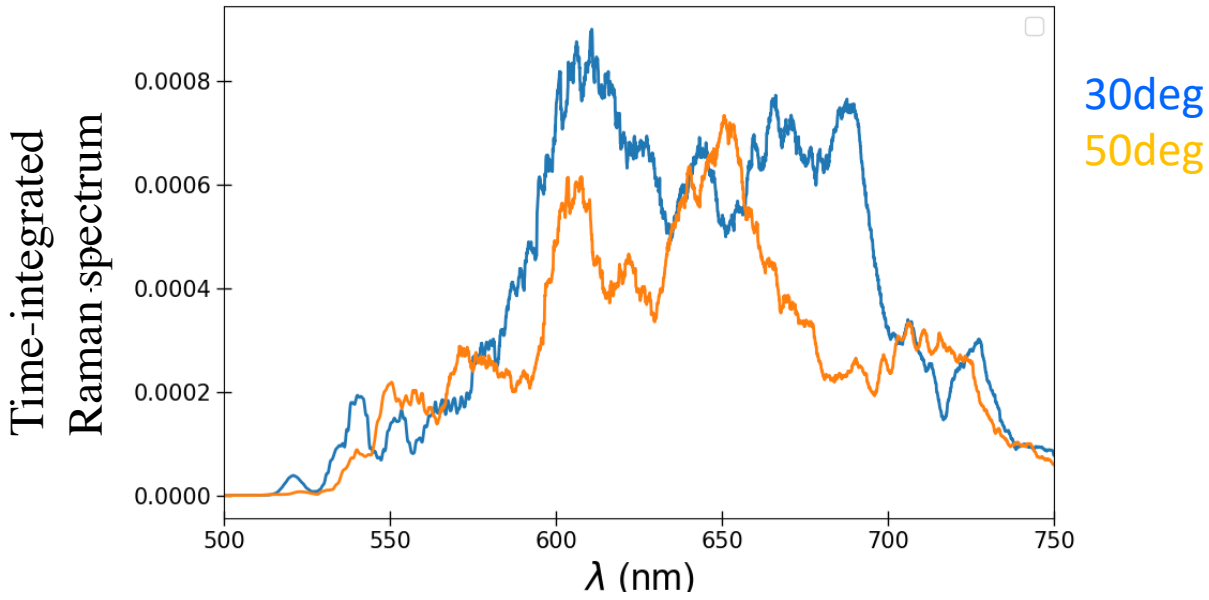

Simulations also indicate wavelength shift is due to Raman refraction

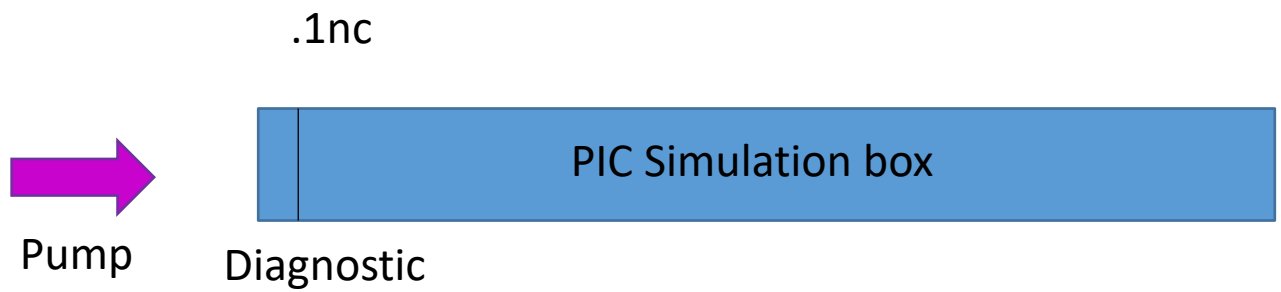

FABS data: clear shift

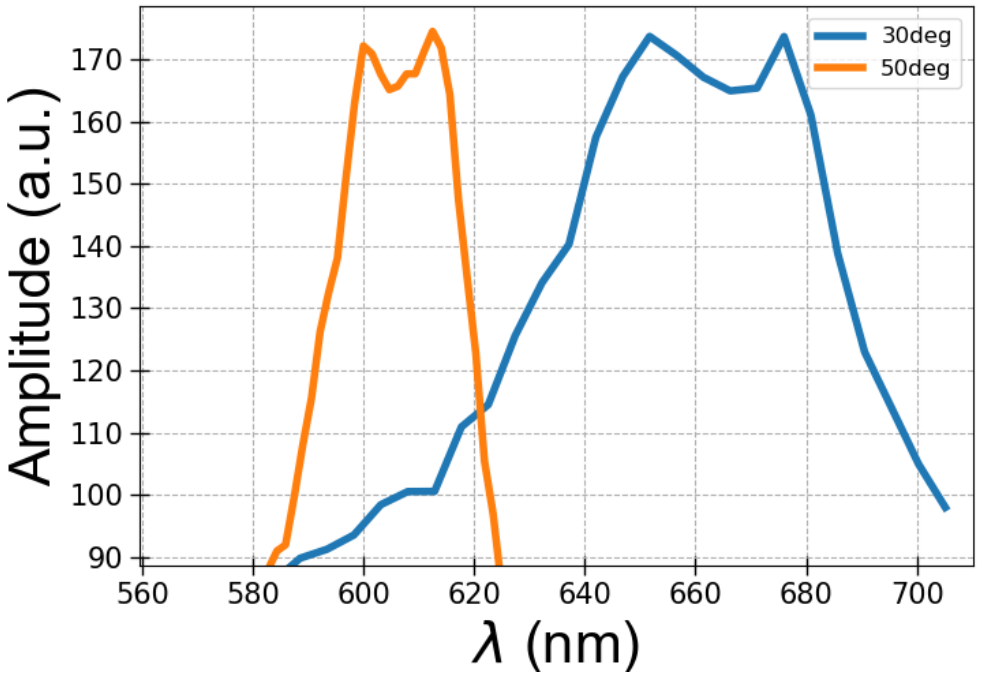

PIC Simulations: no clear shift (refraction not captured)

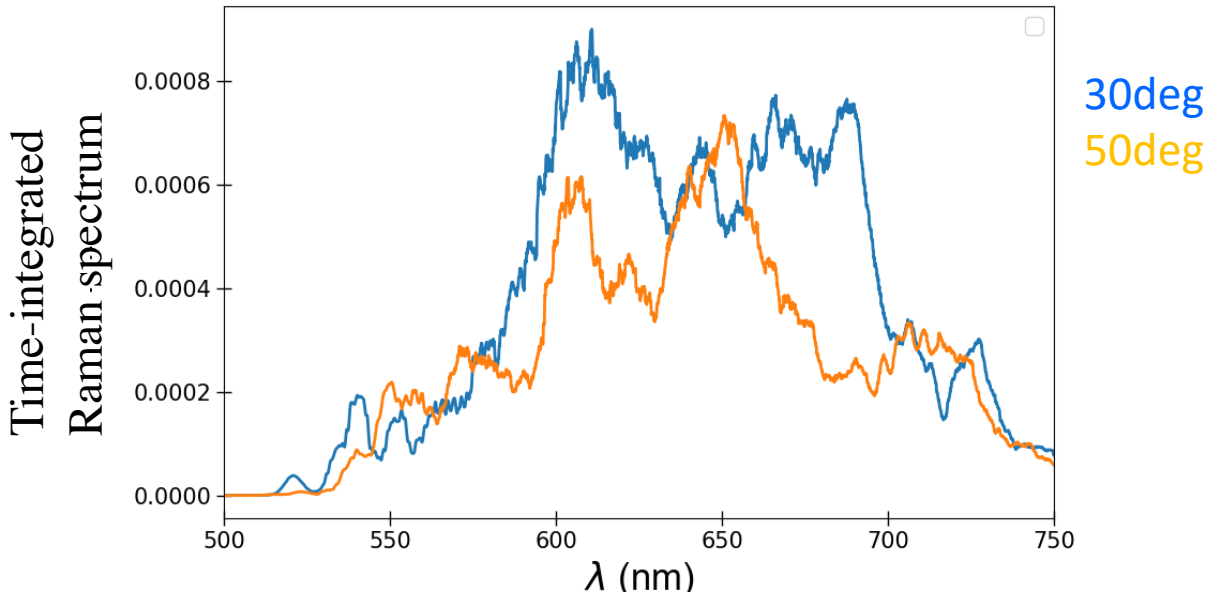

Raman reflectivity is around 3% in PIC simulations, closer to 2.5% corrected reflectivity

Other coupling processes deplete the pump and accelerate electrons

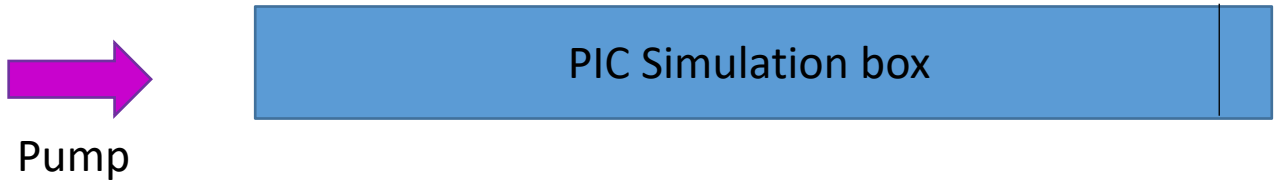

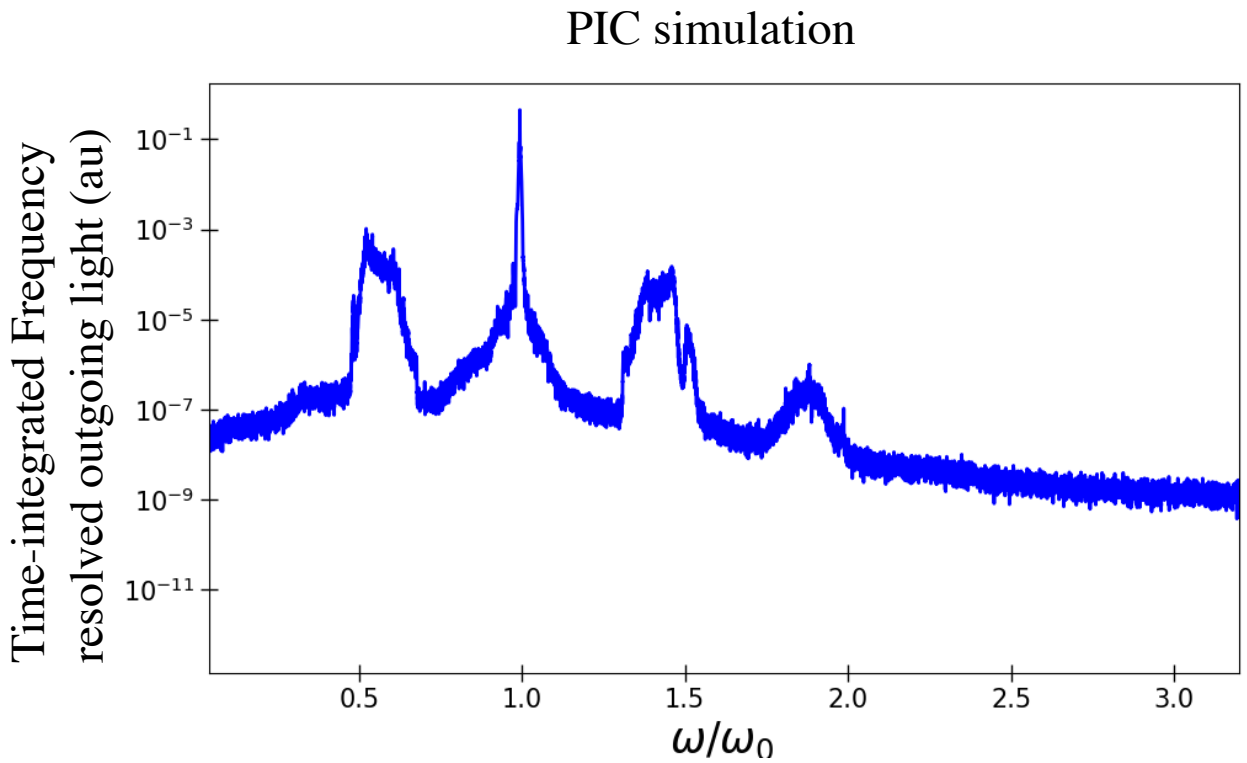

Other coupling processes deplete the pump and accelerate electrons

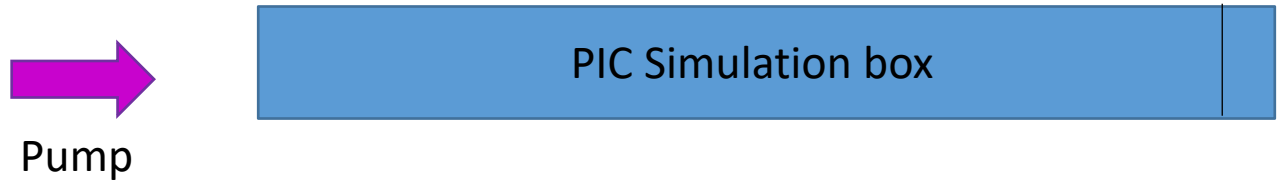

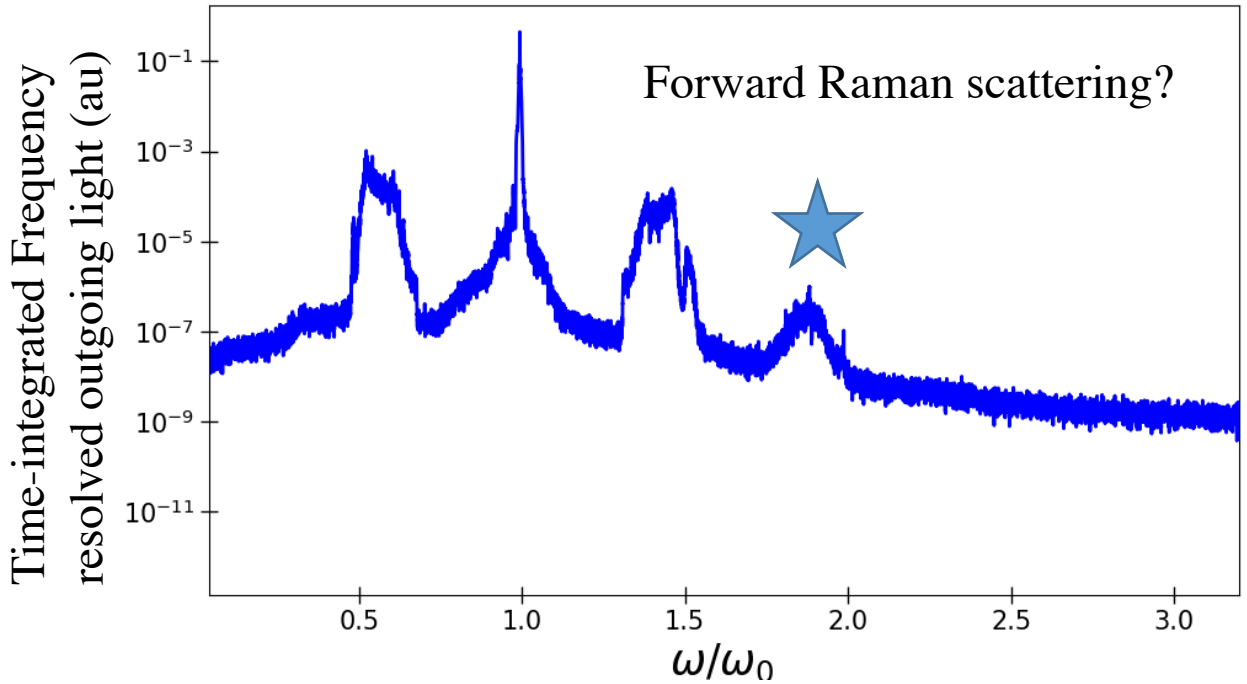

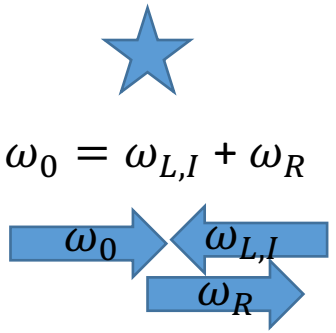

Other coupling processes deplete the pump and accelerate electrons

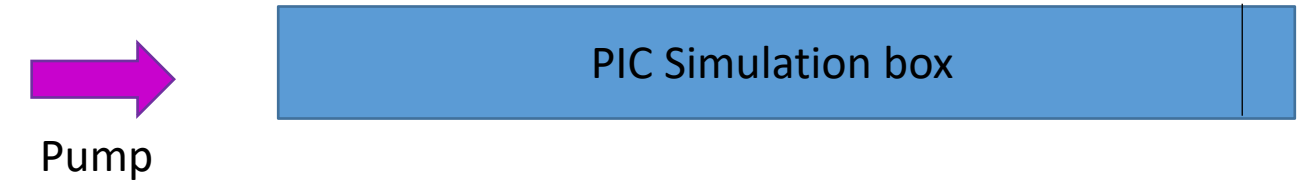

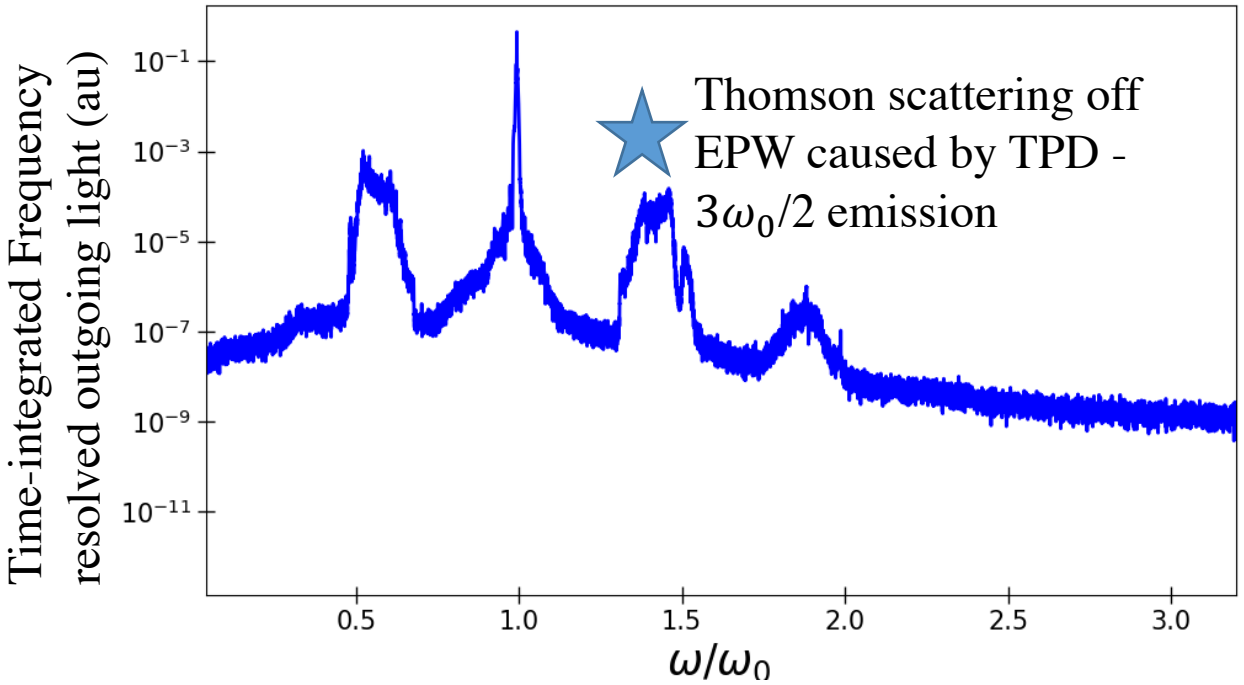

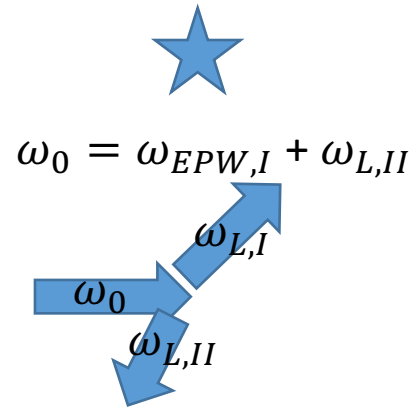

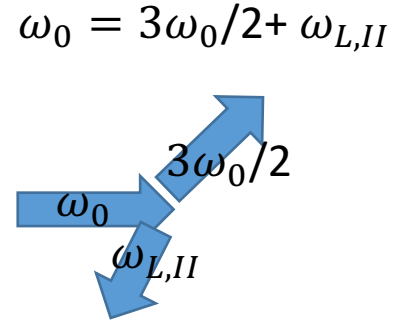

Other coupling processes deplete the pump and accelerate electrons

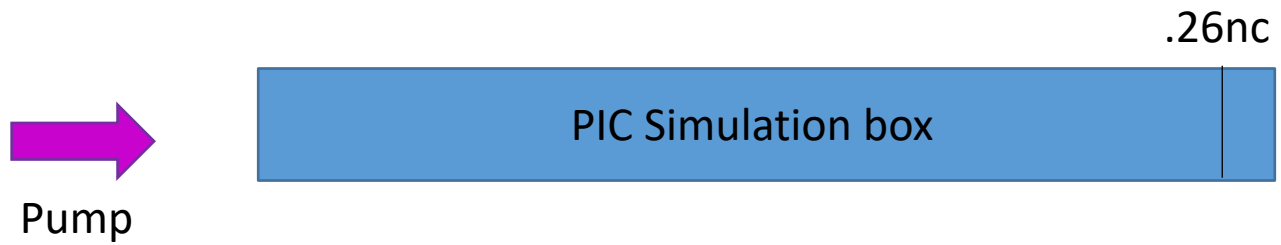

Brillouin scattering of Raman?

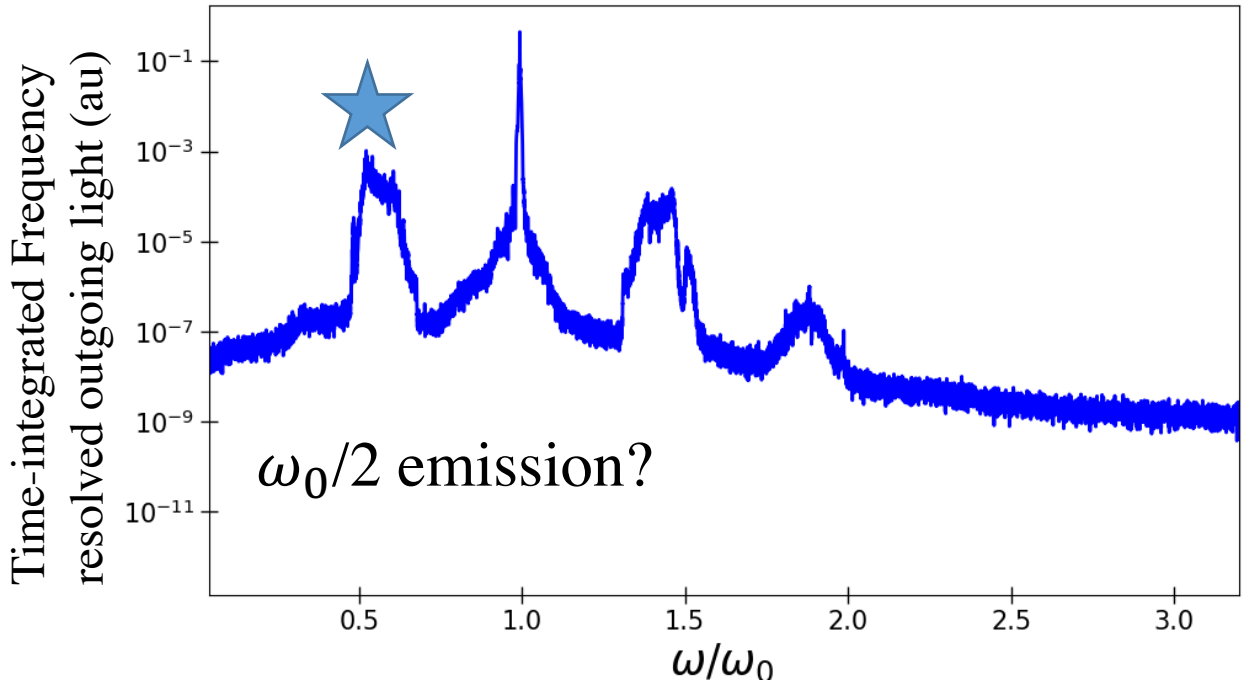

Summary

Laser-plasma instabilities explored at shock-ignition conditions via NIF experiment and simulations

NIF data analysis results:

- Discrepancy between Raman reflectivity and hot electron production
- Diagnostics gives limited information in planar experiments:
  - Raman refraction could be large
  - Side-scattering could be important
- Data showed relevant part of Raman light not detected

Numerical results (preliminary):

- Raman refraction not captured in PIC simulations
- $n_c/4$ activity and rescattering processess deplete pump energy

Summary

Laser-plasma instabilities explored at shock-ignition conditions via NIF experiment and simulations

NIF data analysis results:

- Discrepancy between Raman reflectivity and hot electron production
- Diagnostics gives limited information in planar experiments:
  - Raman refraction could be large
  - Side-scattering could be important
- Data showed relevant part of Raman light not detected

Numerical results (preliminary):

- Raman refraction not captured in PIC simulations
- $n_c/4$ activity and rescattering processes deplete pump energy

Next:

- Hot electrons, evaluation of LPI kinetic aspects
- Parameter scan (laser intensity, laser polarization)
- **We need better diagnostics to measure LPI**

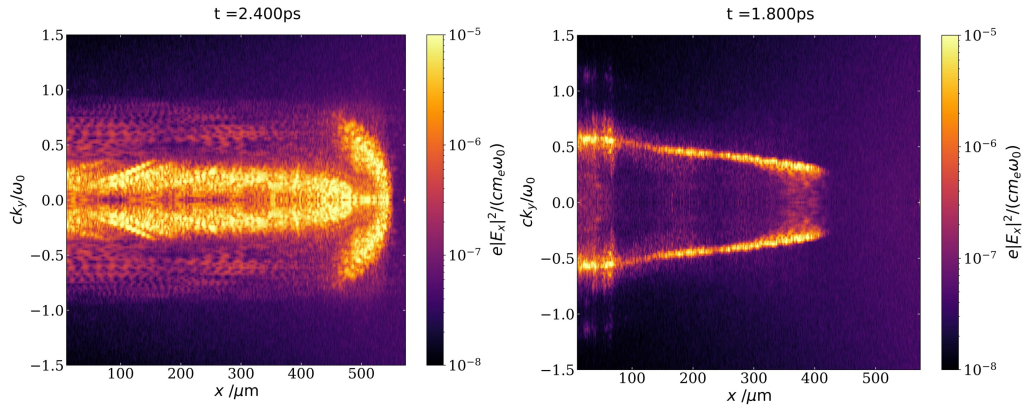

Thank you for your attention

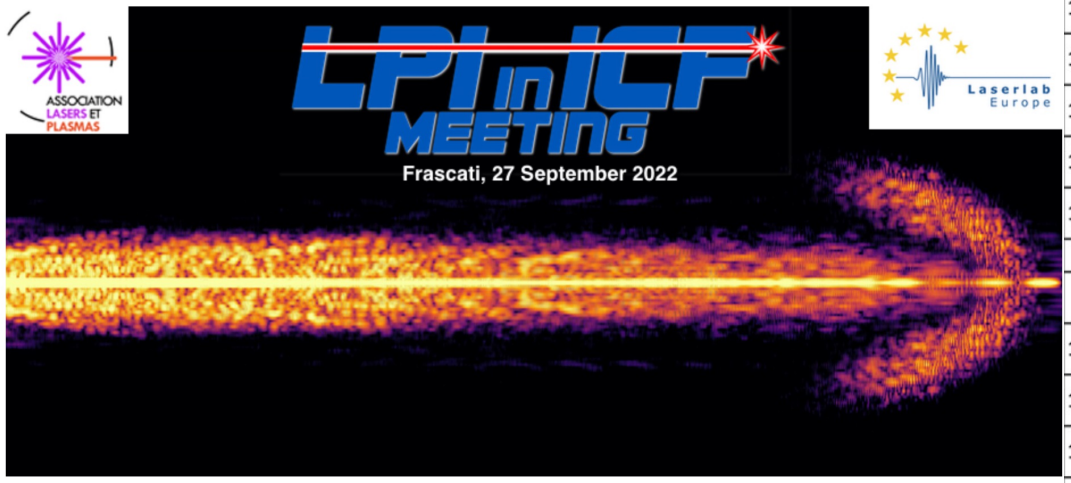

LPI in ICF program

Time (Rome)	SESSION1: LPI reduced models and mitigation techniques Chair: Istvan Foldes	PRESENTERS
9:00-9:10	WORKSHOP OPENING	A. Ruocco - V. Tikhonchuk
9:10-9:30	The Green Option for IFE: STUD Pulses, Learned and Adaptive Control of LPI either to tame or to enhance	Bedros Afeyan
9:30-9:50	Suppression of the stimulated Raman scattering by using a stochastic phase low-coherence laser	Yan Yin
9:50-10:10	Competition between parametric instabilities in inhomogeneous plasma	Zhao Liu
10:10-10:40	COFFE' BREAK	
10:40-11:00	Polychromatic drivers for inertial confinement fusion	Yao Zhao
11:00-11:20	A steady-state approach for modelling laser-plasma instabilities in large scale simulations	Arun Nutter
11:20-13:00	DISCUSSION - Chair: Robbie Scott	
13:00-14:00	LUNCH BREAK	
	SESSION 2: LPI characterization: theory, simulation, experiment, and data-driven models Chair: F. Consoli	
14:00-14:20	Importance of the stimulated Raman side-scattering instability in direct irradiation experiments in the context of Inertial Confinement Fusion	Kevin Glize
14:20-14:40	Explicit high-order symplectic integrators of coupled Schrodinger equations for pump-probe systems	Xiaobao Jia
14:40-15:00	SRS-SBS competition and nonlinear laser energy absorption in a high temperature plasma	Vladimir Tikhonchuk
15:00-15:30	COFFE' BREAK	
15:30-15:50	k-space theory of stimulated Raman and Brillouin side scattering	Chengzhuo Xiao
15:50-16:10	Two plasmon decay instability stimulated by large-incidence-angle lasers in inertial confinement fusion	Rui Yan
16:10-16:40	Influence of random phase plates on the growth of the Backward stimulated Brillouin scatter	Charles Ruyer
16:40-18:00	DISCUSSION - Chair: Vladimir Tikhoncuk	
18:00-18:20	MEETING WRAP-UP	

Polarization scan will provide more information on LPI

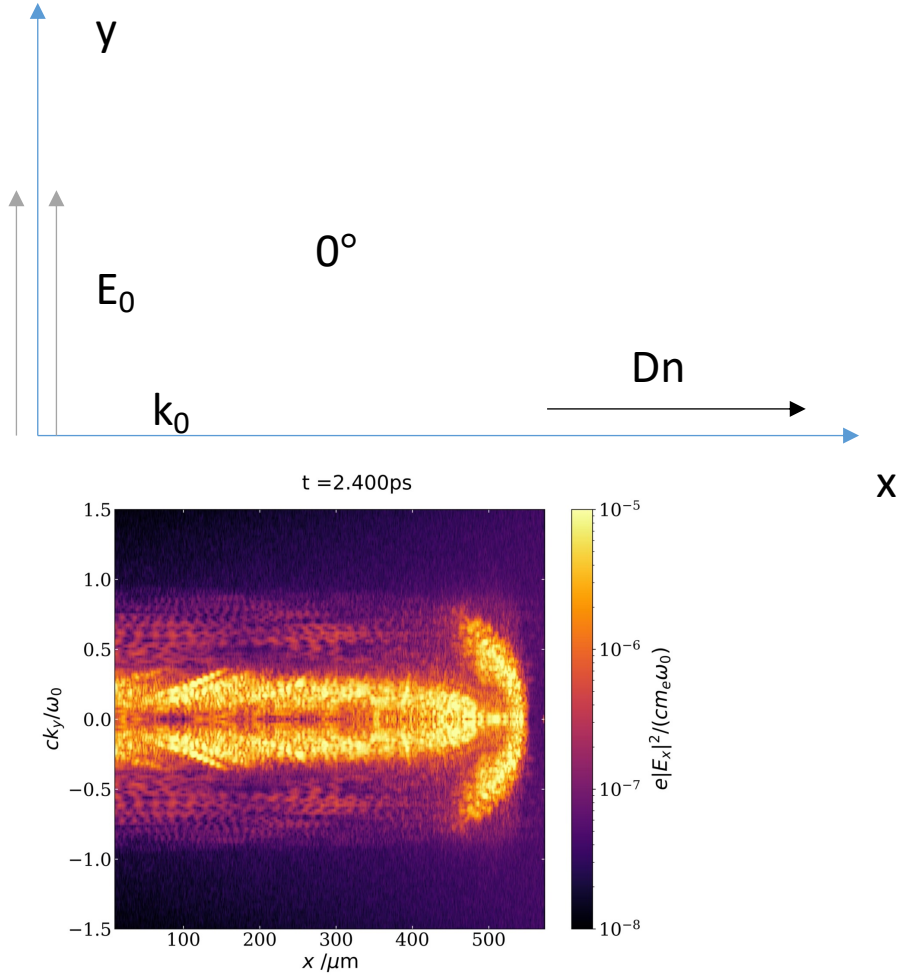

Backscattered (and quasi-back-scattered) Raman TPD

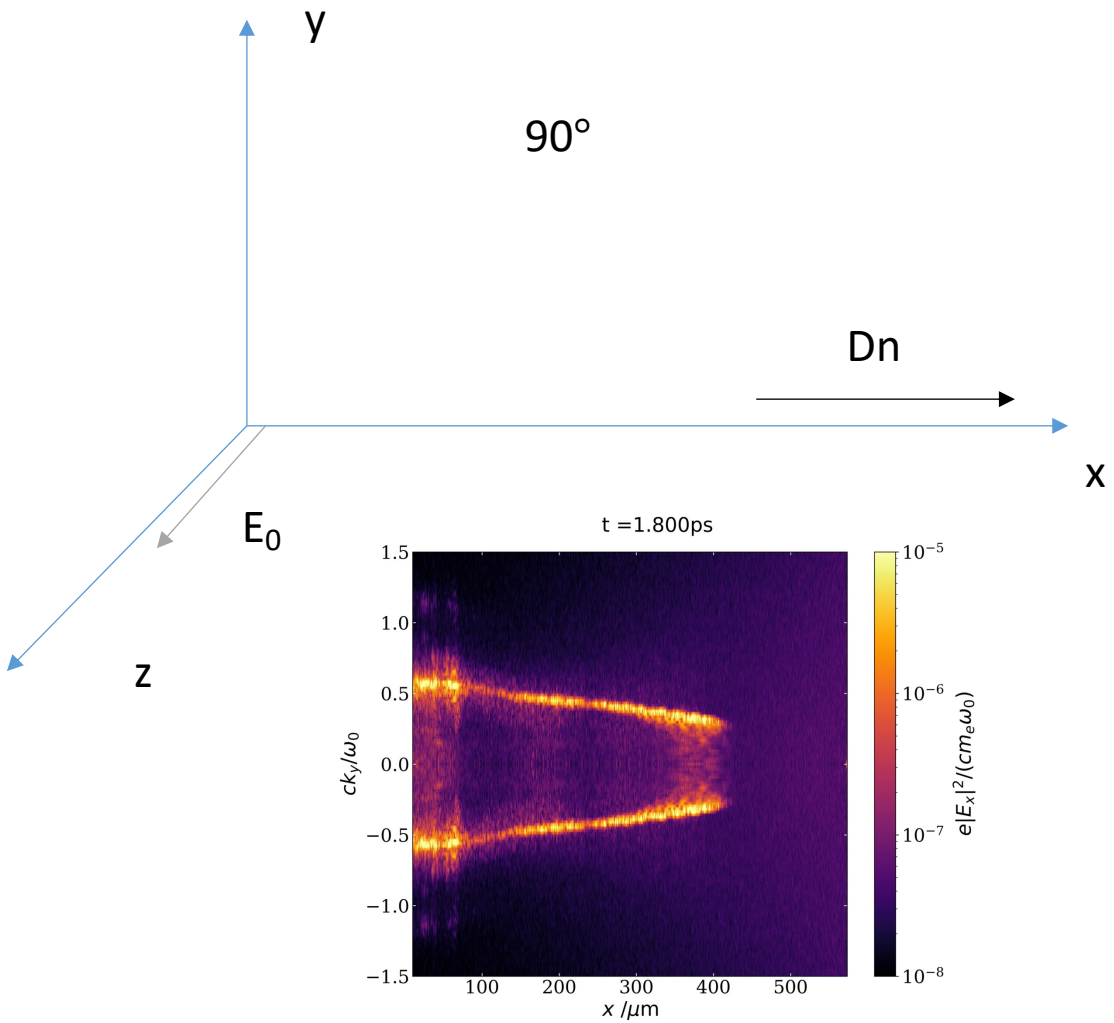

Side-scattered Raman

Polarization scan will provide more information on LPI

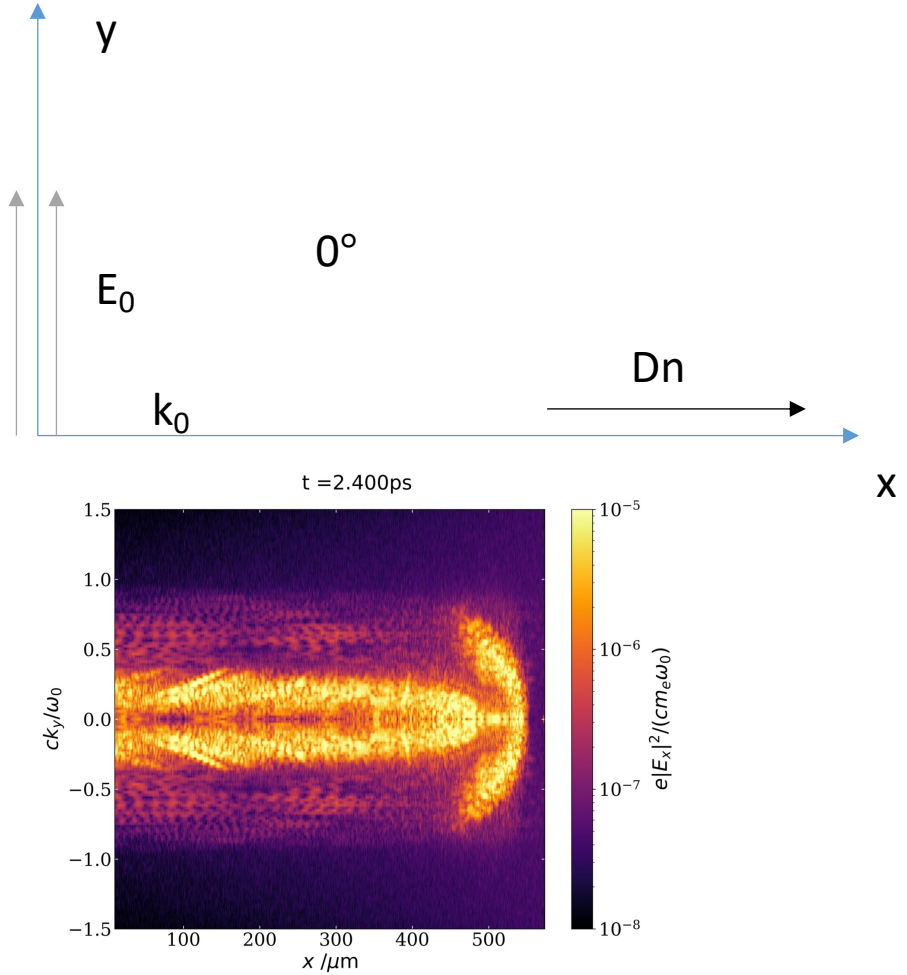

Backscattered (and quasi-back-scattered) Raman TPD

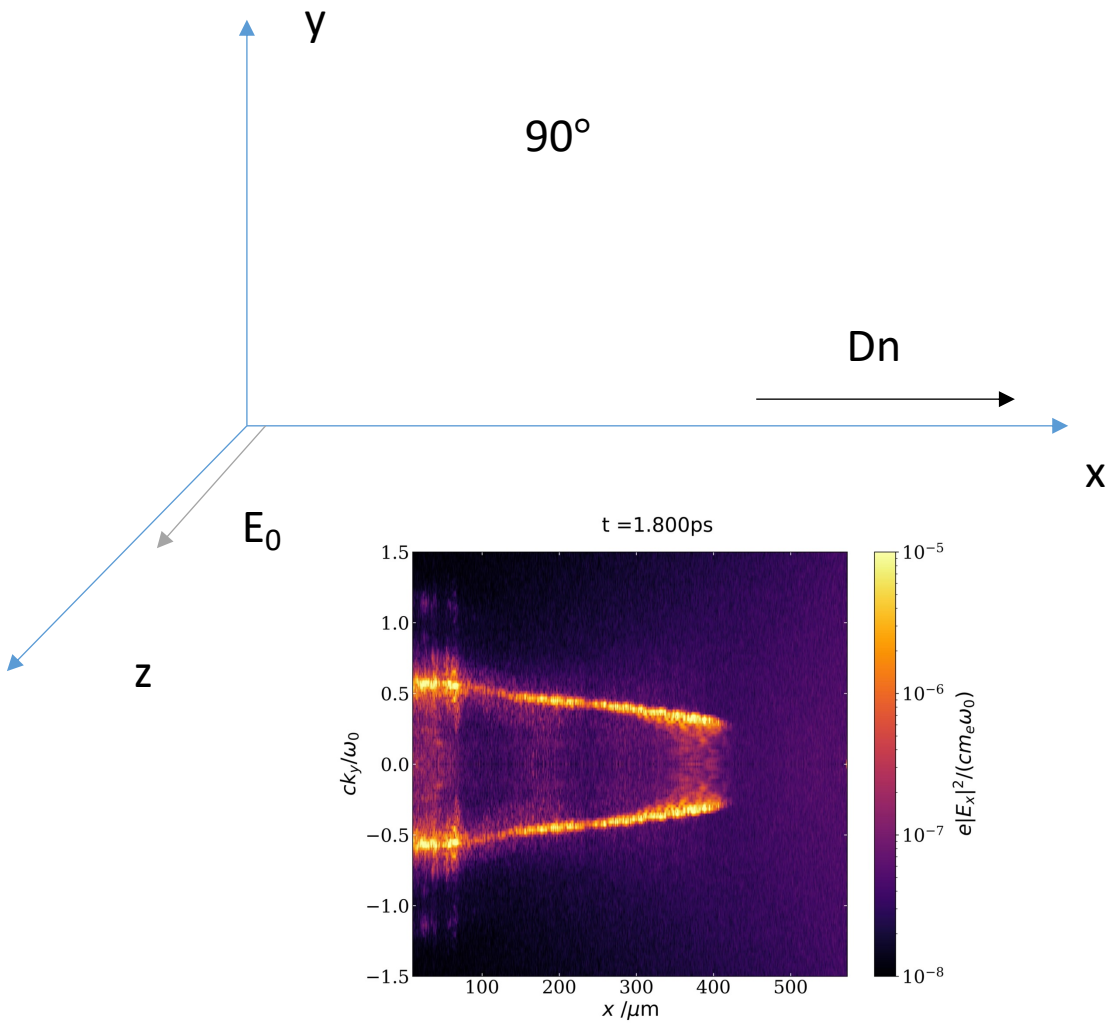

Side-scattered Raman

Polarization scan will provide more information on LPI

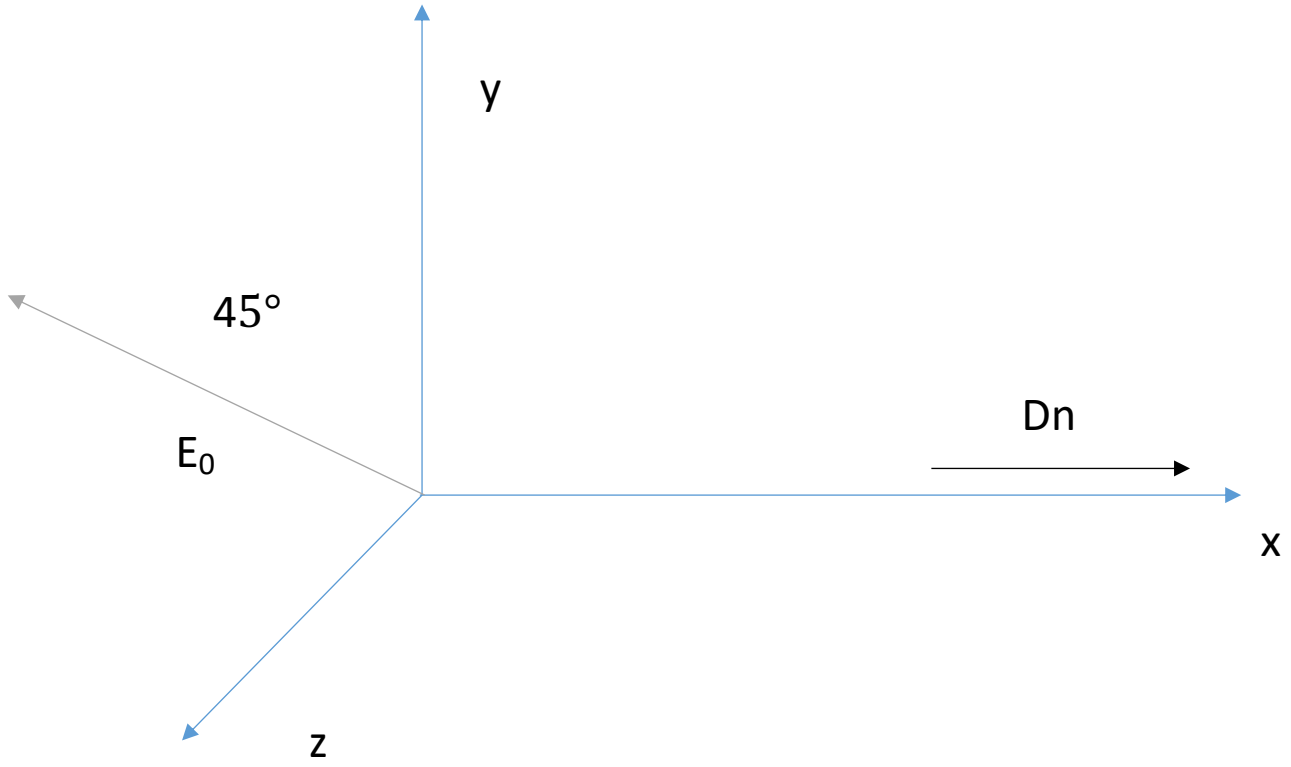

45° polarization: E_0 has components along y and z

Polarization scan will provide more information on LPI

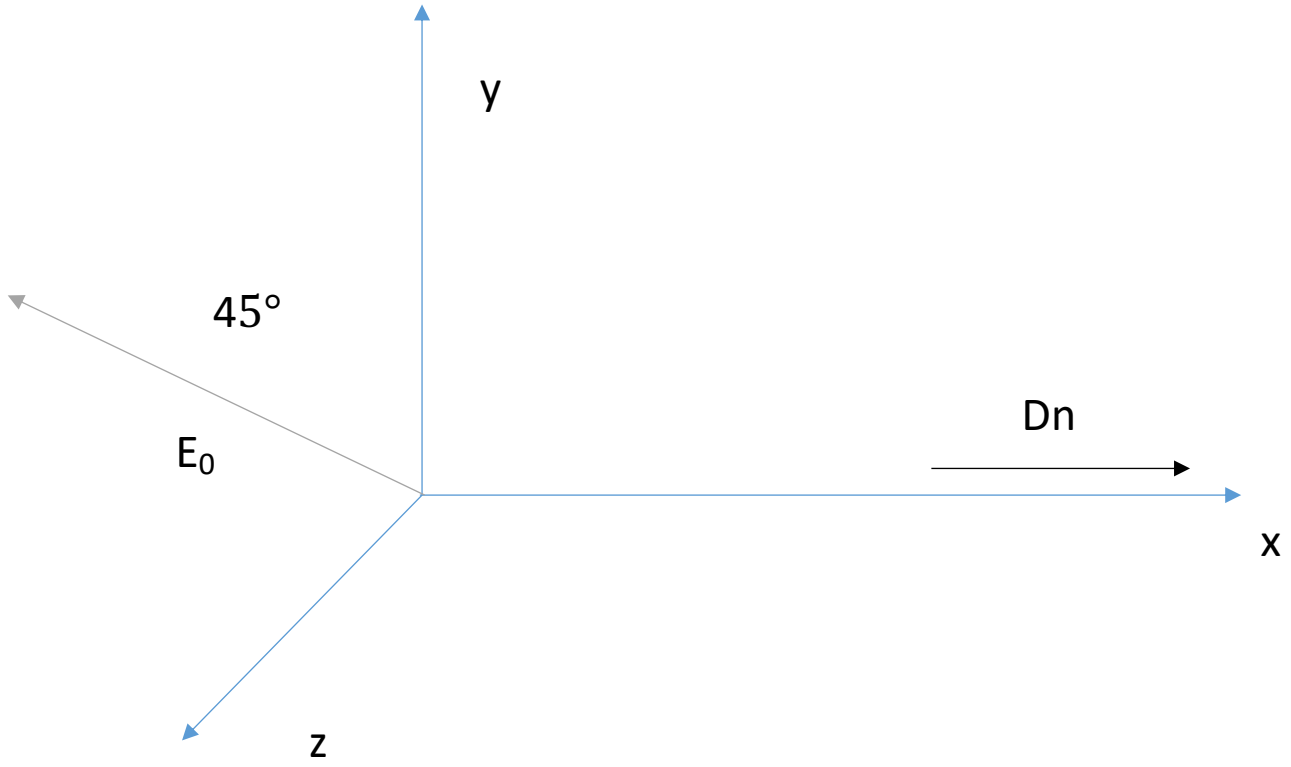

45° polarization: E_0 has components along y and z

Simulations join the effort to tackle LPI at ignition conditions

Seaton, PoP **27**, 082704 (2020)

	Scatter fraction $f_{scatter}$ (/%)			Diverted fraction f_{div} (/%)			Hot electron fraction f_{hot} (/%)		
Simulation	bSRS	SBS	Total	bSRS	TPD	Total	25–100 keV	>100 keV	>25 keV
OMEGA-scale	0.5	0.8	1.3	1.1	72.7	74.6	31.0	11.2	42.3
NIF-scale	23.5	18.9	42.4	47.0	24.1	89.9	26.7	11.2	37.9

L_n = 600 um – I_0 = 2x10^{15} W/cm^2 – λ_0 = 0.35 um - T_e = 4 keV

Ji, MRE 6, 015901 (2021)

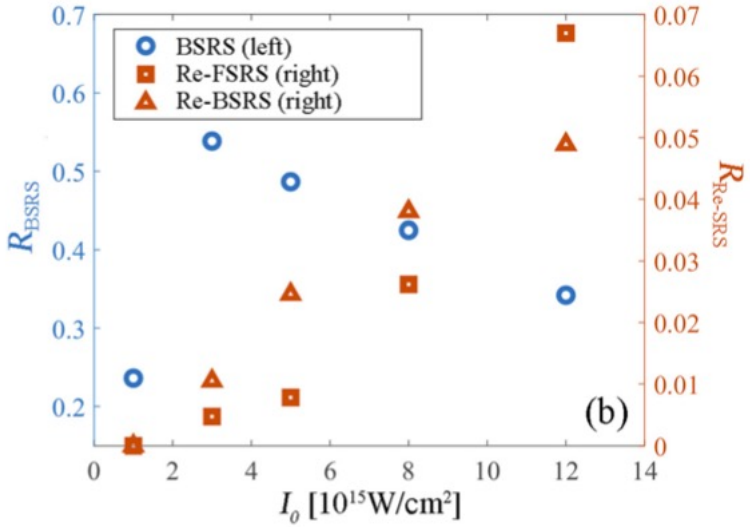

L_n = 1800 um – I_0 = 1.2x10^{16} W/ cm^2 – λ_0 = 1.05 um - T_e = 1 keV

Planar targets have been used for LPI experiments at shock-ignition conditions on OMEGA

Scott, PRL 127 (6), 065001 (2021)

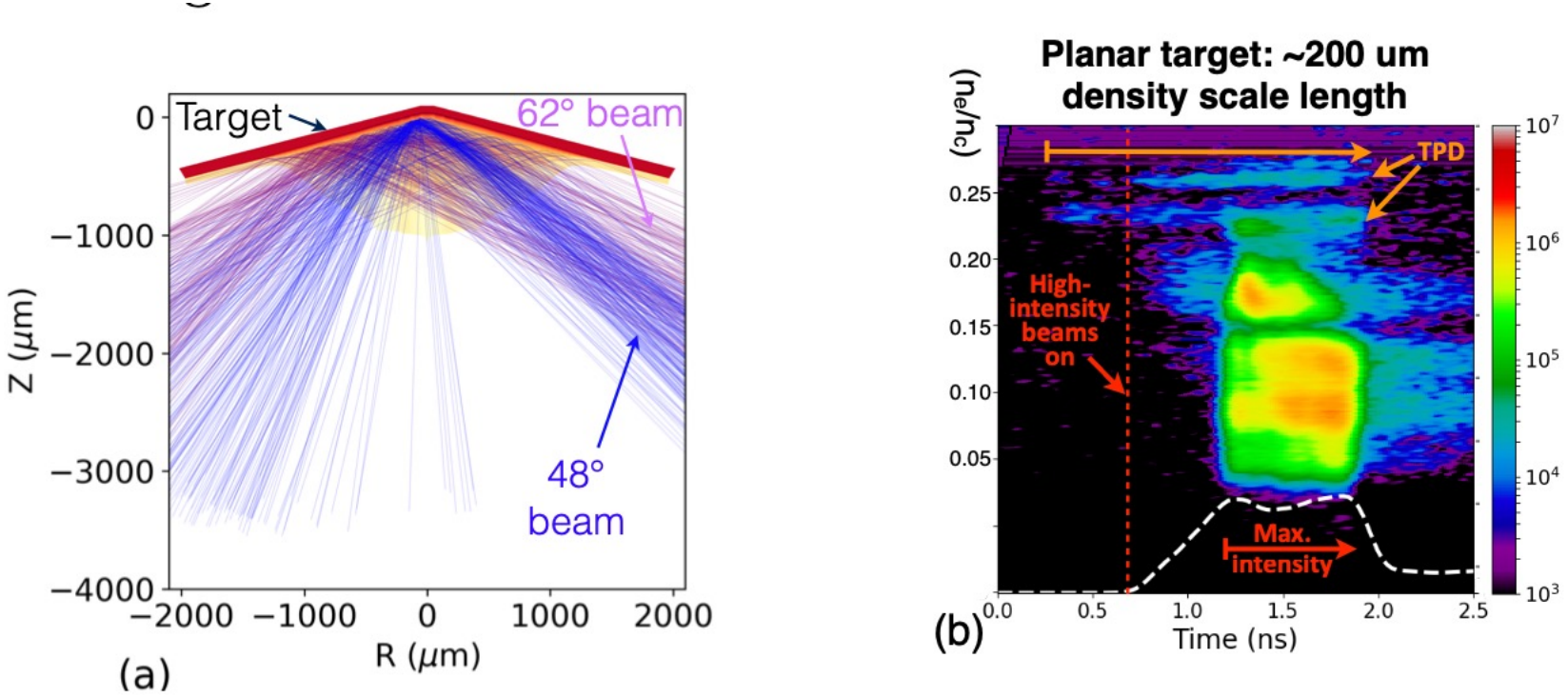

L_n = 200-500 um – $I_0 = 10^{16}$ W/ cm^2 – λ_0 = 0.35 um - T_e = 3 keV

Planar targets have been used for LPI experiments at shock-ignition conditions on OMEGA

Scott, PRL 127 (6), 065001 (2021)

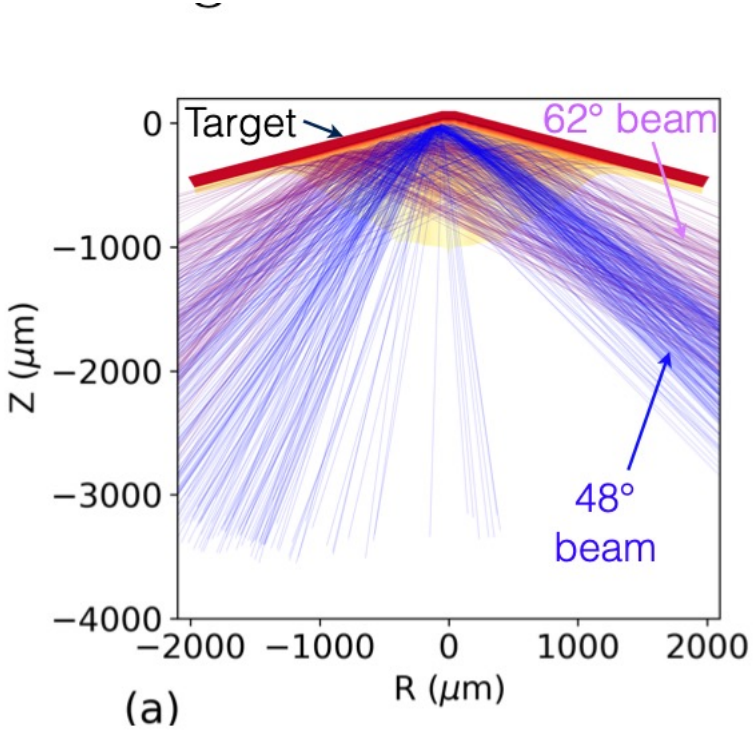

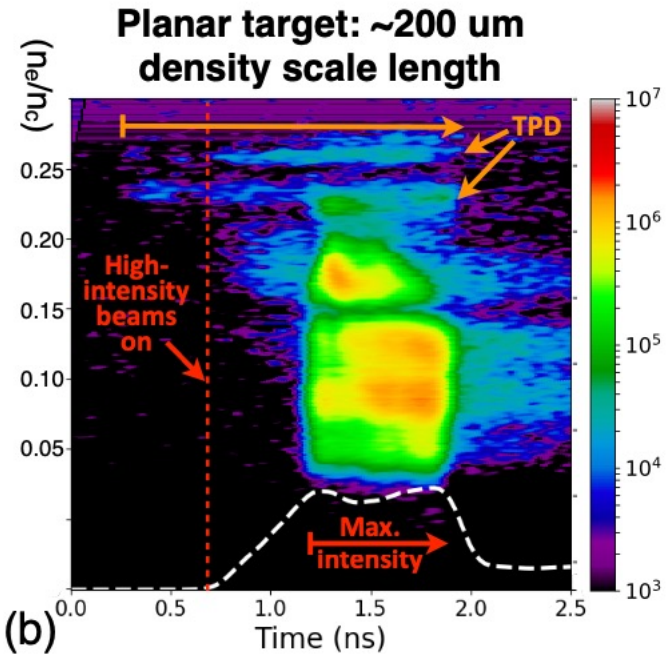

L_n = 200-500 um – $I_0 = 10^{16}$ W/ cm^2 – λ_0 = 0.35 um - T_e = 3 keV

$L_n > 600$ um – $I_0 = 10^{16}$ W/ cm^2 – λ_0 = 0.35 um - $T_e > 6$ keV

Side-scattering Raman signal informs us on plasma temperature

Estimated electron temperature from hydro sims at 7.5 ns: 3 keV

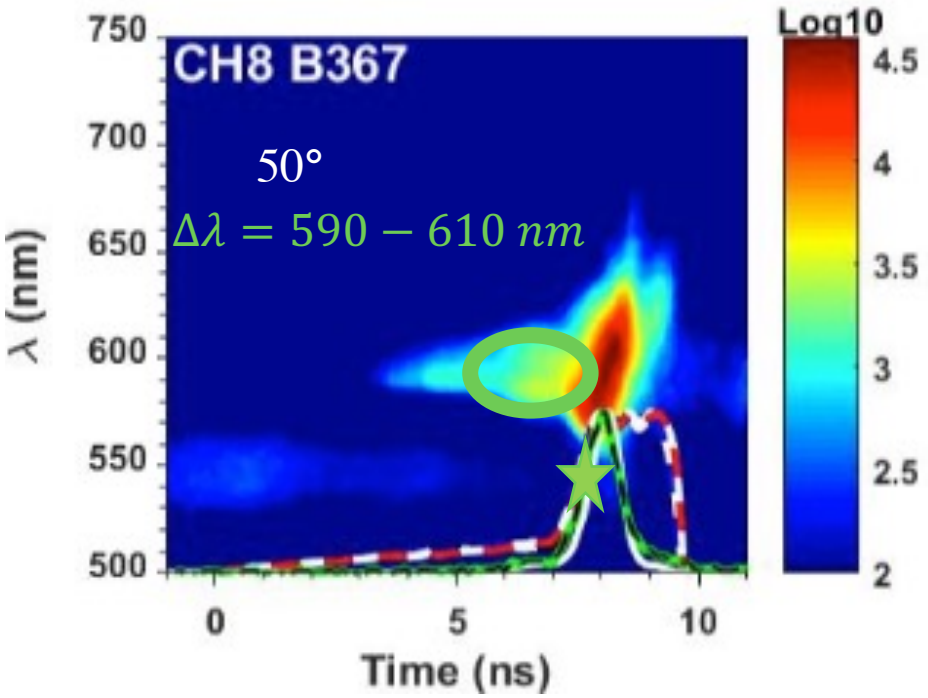

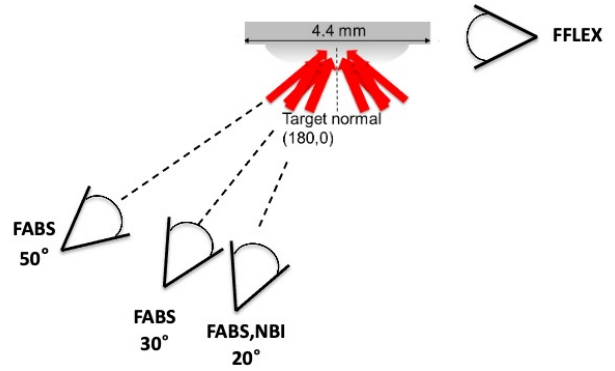

Side-scattering Raman signal informs us on plasma temperature

Estimated electron temperature from hydro sims at 7.5 ns: 3 keV

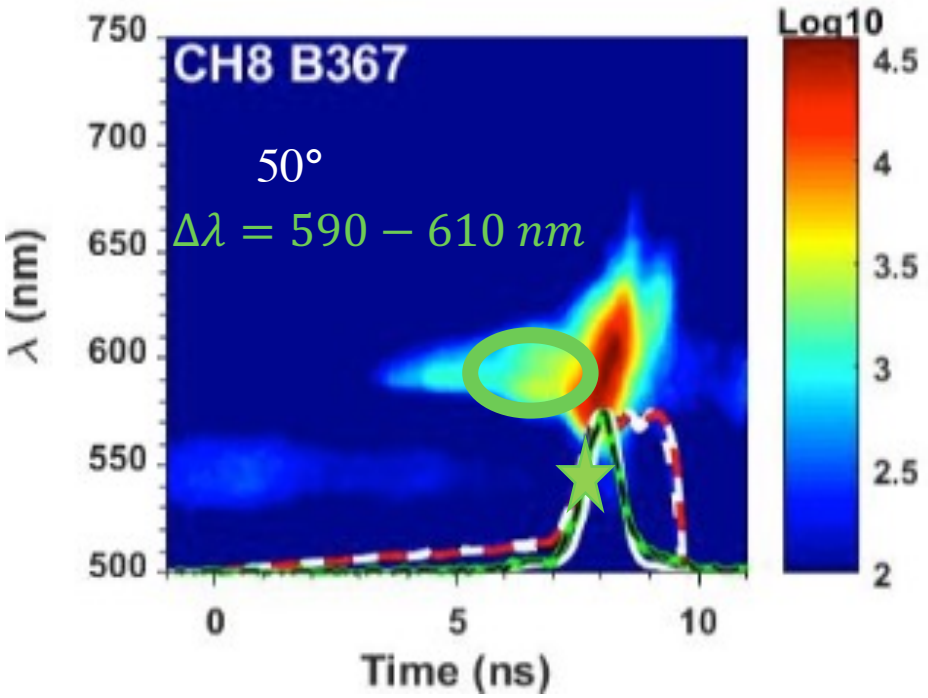

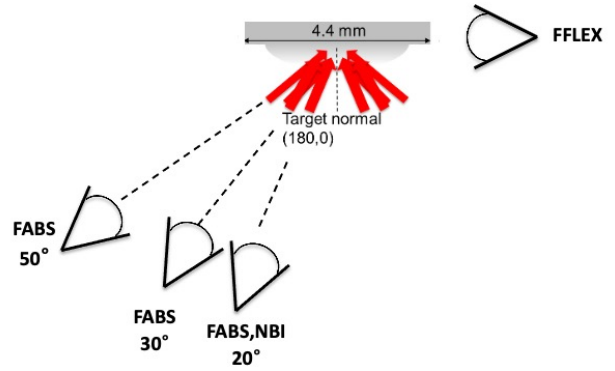

$$\sin(\theta_{\text{out}}) = \sqrt{1 - \omega_{pr}^2/\omega_s^2}$$ *

*Michel, PRE **99**, 033203 (2019)

Side-scattering Raman signal informs us on plasma temperature

Estimated electron temperature from hydro sims at 7.5 ns: 3 keV

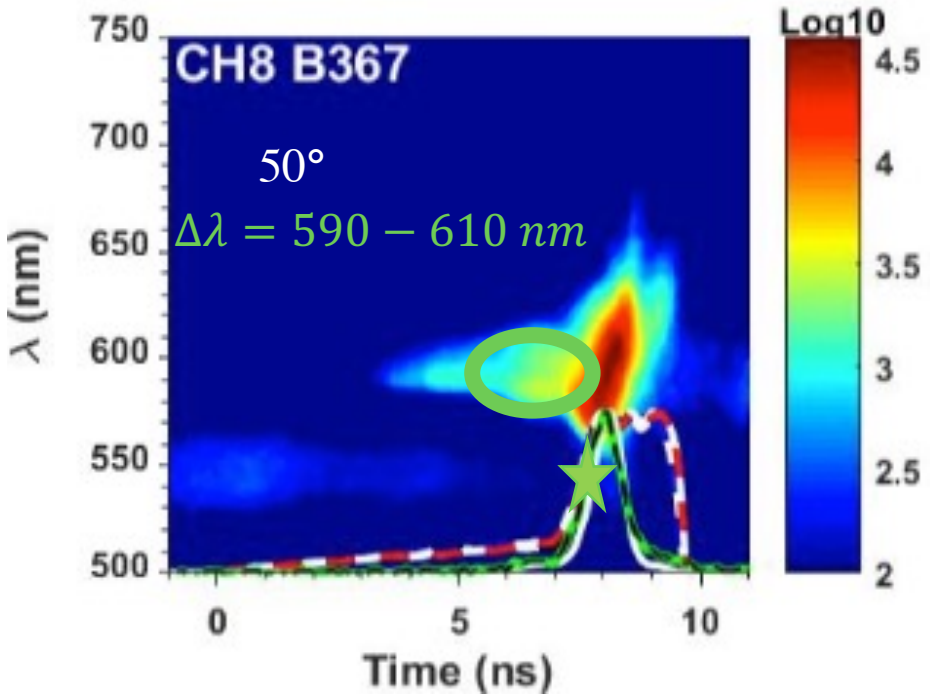

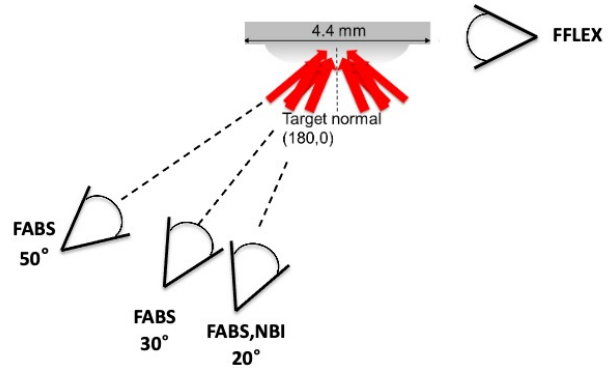

$$\sin(\theta_{\text{out}}) = \sqrt{1 - \omega_{pr}^2/\omega_s^2}$$ *

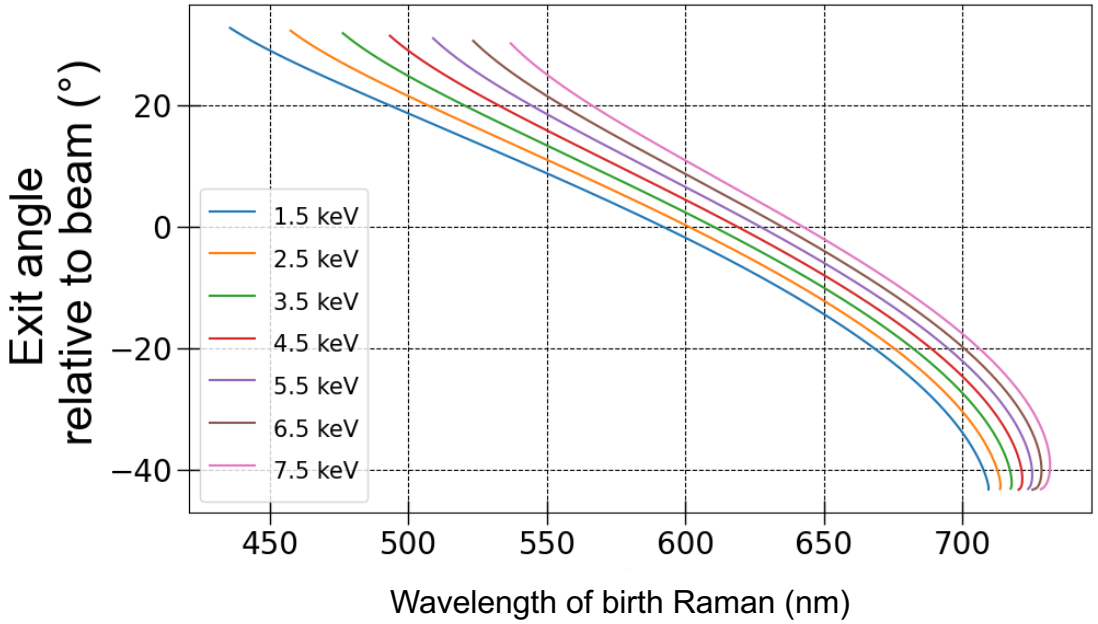

*Michel, PRE **99**, 033203 (2019)

Side-scattering Raman signal informs us on plasma temperature

Estimated electron temperature from hydro sims at 7.5 ns: 3 keV

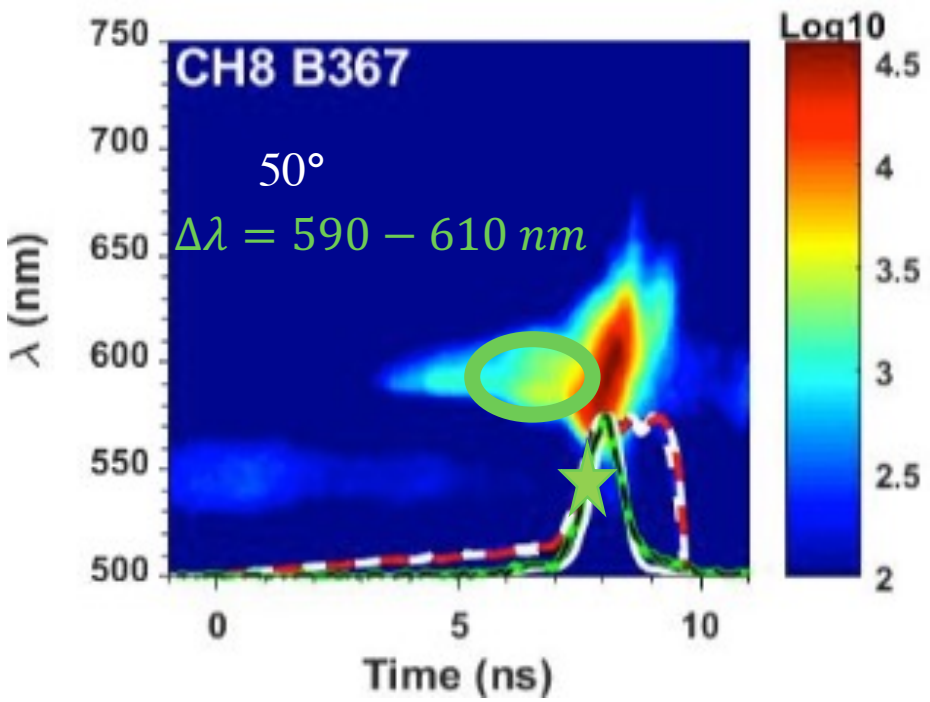

$$\sin(\theta_{out}) = \sqrt{1 - \omega_{pr}^2/\omega_s^2}$$ *

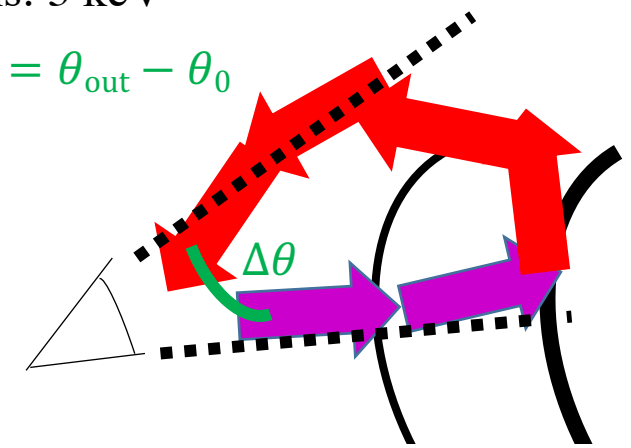

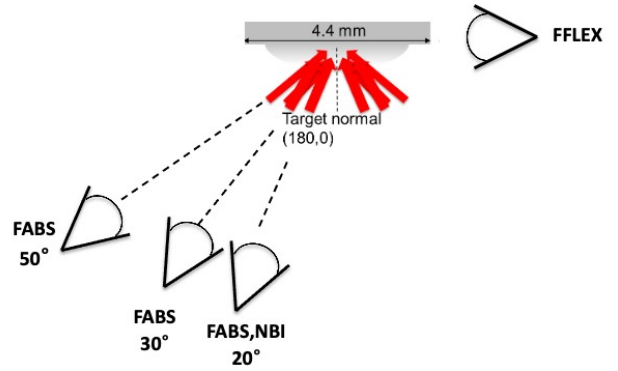

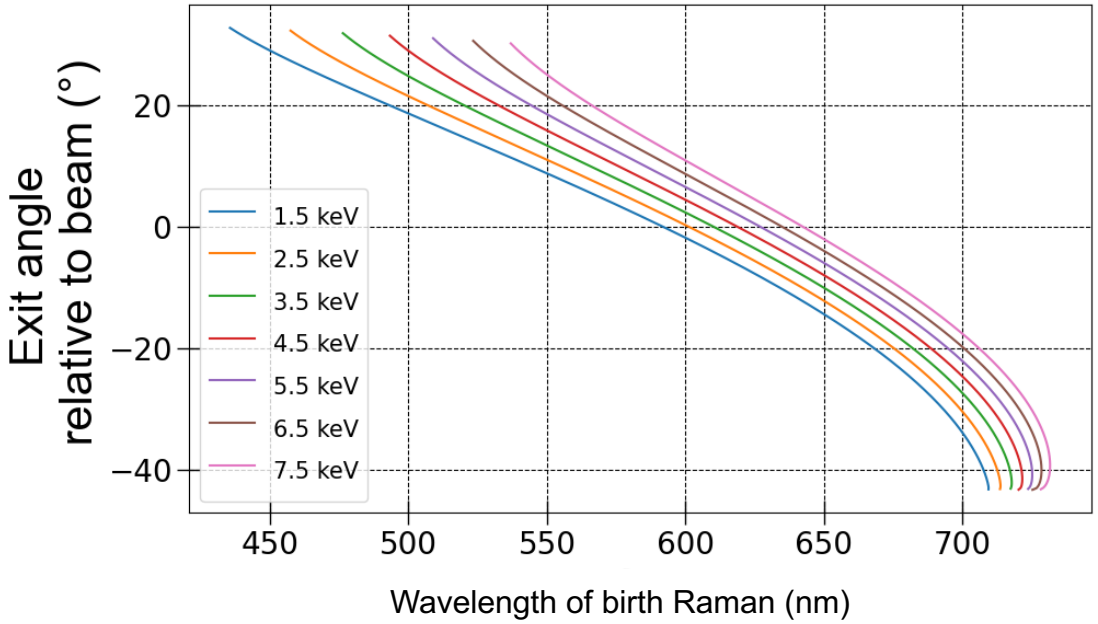

*Michel, PRE **99**, 033203 (2019)

Side-scattering Raman signal informs us on plasma temperature

Estimated electron temperature from hydro sims at 7.5 ns: 3 keV

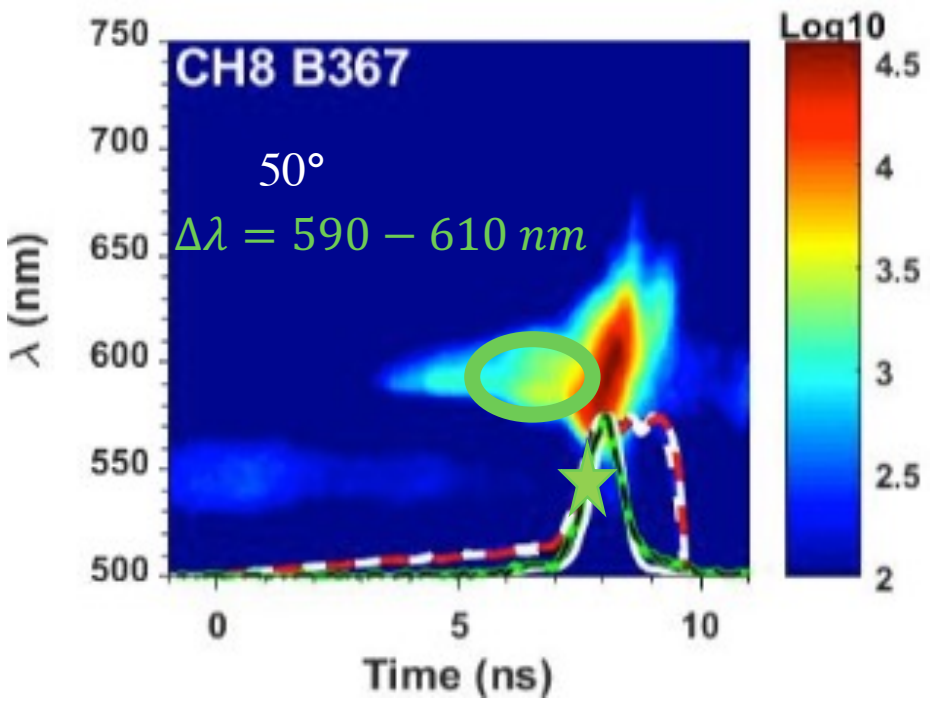

$$\sin(\theta_{\text{out}}) = \sqrt{1 - \omega_{pr}^2/\omega_s^2} \quad *$$

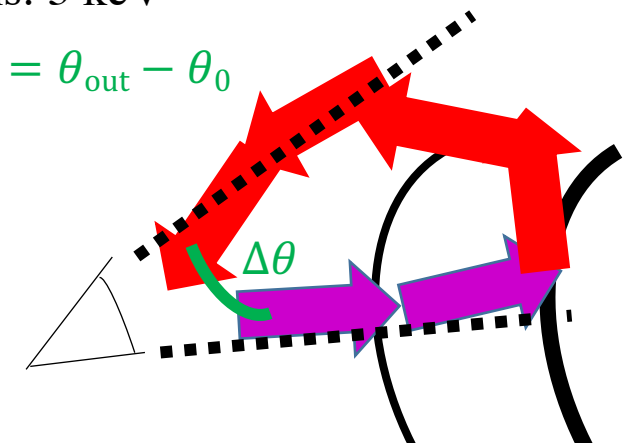

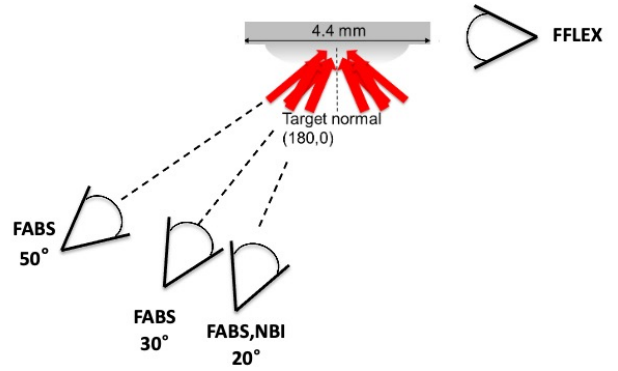

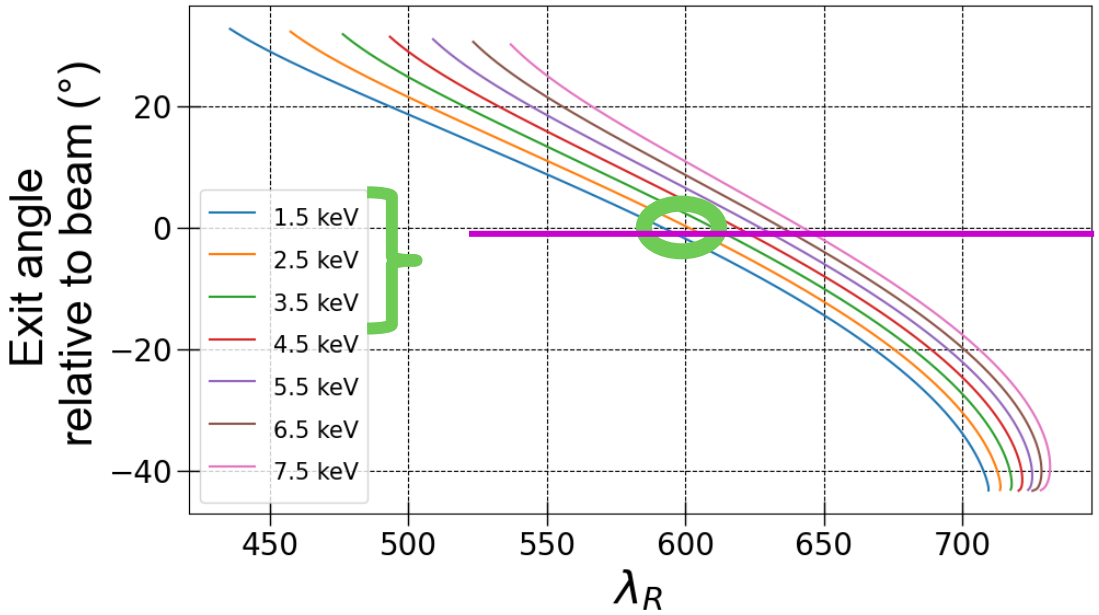

*Michel, PRE **99**, 033203 (2019)

Good agreement between FABS and hydro result

Polarization scan will provide more information on LPI importance